Frequency Sub-Carrier Based Adaptive Technique for OFDM Systems with Antenna Arrays

by

Stipe Moric

A thesis submitted in conformity with the requirements
for the degree of Masters of Applied Science
Graduate Department of Electrical and Computer Engineering
University of Toronto

Your file Votre référence
ISBN: 0-612-95351-3
Our file Notre référence
ISBN: 0-612-95351-3

Abstract

Frequency Sub-Carrier Based Adaptive Technique

for OFDM Systems with Antenna Arrays

Stipe Moric

Masters of Applied Science

Graduate Department of Electrical and Computer Engineering

University of Toronto

2004

Orthogonal frequency division multiplexing (OFDM) is gaining considerable attention and is a viable candidate in future broadband wireless communication systems. However as more devices become wireless in a limited frequency environment, high powered co-channel interference suppression techniques become increasingly important. In this regard adaptive arrays have been incorporated into OFDM schemes to further increase capacity and robustness of the overall system.

We introduce here a new method to extend spatial processing techniques to mitigate high powered co-channel interference in an orthogonal frequency division multiplexing system. The proposed algorithm uses optimal weights determined from classical methods, and known frequency information, to formulate adaptive weights specific to each sub-carrier. Performance improvements are investigated through computer simulations. These simulations in near-far scenarios illustrates the importance of such a technique.

Dedication

This work is dedicated to my parents

Acknowledgements

First and foremost I would like to extend my sincere gratitude to my supervisor, Dr. Raviraj Adve, for giving me this opportunity. If it wasn't for your patience and understanding none of this would have become a reality. I appreciate your invaluable guidance, support and encouragement.

I would also like to extend my gratitude to the other members of the communications group who assisted me throughout my thesis. Especially the Amir's, Wei, Adam, Ela, Rebecca and Ramy. Each one of you contributed valuable insight when it was most needed.

Finally I would like to thank the support group that surrounded me and stood by me during this time, my parents, family and friends. I know it wasn't always easy to be around me, but I appreciate your empathy.

Contents

List of Tables

List of Figures

Chapter 1

Introduction

1.1 Introduction and Motivation

Fourth generation (4G) mobile communication systems call for technology that can deliver high data rates and seamless connectivity. Higher data rates will provide the user with more services at a higher quality such as sending and receiving video, voice, data, and games over the wireless network. A natural choice to achieve high data rates is to employ broadband systems. However, because of limited available frequency spectrum worldwide, efficient spectrum utilization techniques are required.

Orthogonal frequency division multiplexing (OFDM), has become one of the prime candidates for 4G mobile technology and ad-hoc networks, because of its ability to achieve high-data rates and immunity to frequency-selective fading in multi-path environments [1–4]. In Europe, OFDM is already accepted as the standard for digital video broadcasting (DVB) and digital audio broadcasting (DAB) [5]. The IEEE 802.11a and IEEE 802.11g include OFDM based standards [6]. Recently Texas Instruments has announced wONE, a universal router technology, that delivers IEEE 802.11a and IEEE 802.11g operations from a single chipset, finally making these standards affordable for mass production. Also OFDM is accepted for high performance LAN type 2 (Hiperlan/2) [7], and

mobile multimedia access communications (MMAC) systems. There is no denying the increasing popularity of OFDM based systems. However, this popularity brings with it the problem of interference limiting the performance of OFDM systems. Techniques to mitigate high powered co-channel interference caused by wireless LAN's, jammers, and the near-far effect of ad-hoc networks are therefore required.

Adaptive antenna arrays have also gained considerable attention because of their ability to increase data throughput and lower the the probability of outage without allocating additional frequency spectrum [8]. In addition, spatial processing techniques along with multiple element antennas provide interference suppression capabilities by exploiting the spatial characteristics of received signals. Combining OFDM systems with adaptive antenna arrays is a logical choice for 4G mobile technology. However, little work dealing with mitigating high-powered co-channel interference in OFDM systems is available. A significant problem with available proposed schemes is that they are extremely computationally intensive [9–12]. This provides the motivation for this thesis research.

This thesis presents a novel algorithm to mitigate high powered co-channel interference in OFDM systems with adaptive antenna arrays. Using known frequency bin information and the optimal weights of one narrowband beamformer, individual weights for each sub-carrier are constructed. This frequency sub-carrier based (FSB) technique is significantly less complex and innovative when compared to other proposed interference suppression schemes. As with other work in this area, we generally assume line of sight communications.

1.2 Contributions

Some of the major contributions of this thesis are listed below.

- Introduce a new effective co-channel interference suppression technique, based

on an innovative scheme to extend classical adaptive weight algorithms. Simulations for various system models and channels are investigated.

- A method to model steering vectors for broadband systems is presented. Previously the steering vector was formulated based on the center frequency, which is not an exact representation.
- Performance limitations of the minimum mean square error adaptive weight technique are studied for broadband systems. Null deviation is investigated for large bandwidths.

1.3 Related Work

A number of techniques for OFDM co-channel interference suppression exists in the published literature [13–18]. However, relatively few research papers focus on high powered co-channel interference, i.e. the near-far problem. Typically two categories of strong interference suppression techniques exist in literature. The first category mitigates the interference using an architecture model of a narrowband beamformer known as a wideband beamformer [9] [10]. The second category uses redundancy in the transmission data to create a more robust OFDM system [11] [12]. Both categories use limited innovation and performance improvements are achieved because a type of repetition created as part of the processing techniques.

1.3.1 Wideband Beamformer

To develop adaptive spatial processing for OFDM systems, researchers have proposed wideband beamforming schemes to mitigate high powered co-channel interference [9] [10]. These techniques generally comprise of a narrowband beamformer, reevaluated for each sub-carrier where individual beamformers optimally adjust weights based on a certain performance criteria.

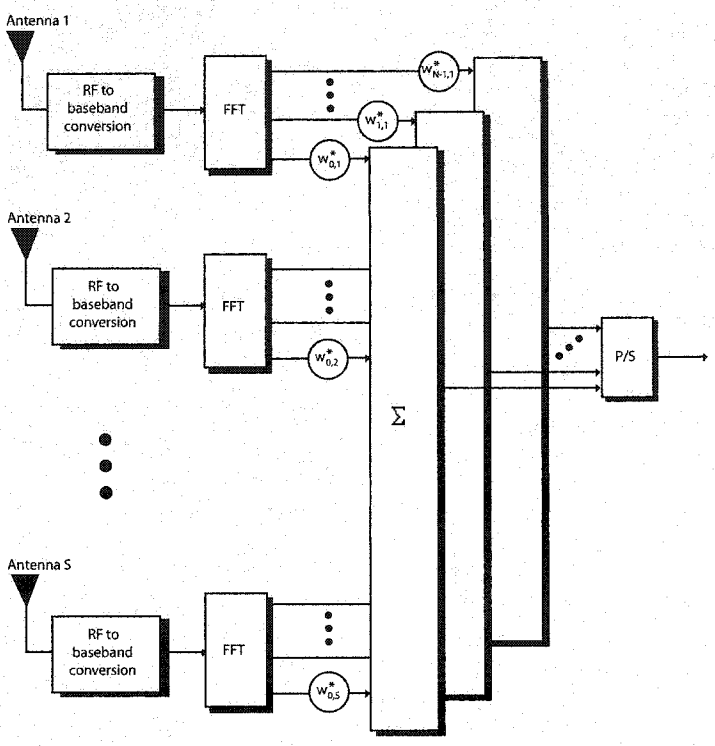

Figure 1.1: A block diagram of a wideband beamformer

The foundation for this procedure is based on the fact that distinct fading and distortion may be present across different sub-carriers of the transmitted OFDM symbol. Therefore a single set of weights will not be able to produce optimal interference suppression across the entire spectrum. By using a narrowband beamformer for each sub-carrier, optimal interference mitigation is achieved. A block diagram of a wideband beamformer is shown in Figure 1.1. It should be stated that the wideband beamformer is a frequency domain beamforming technique.

The wideband beamforming method, however, suffers from larger computational complexity. To reduce the complexity of the wideband beamformer, sub-carrier clustering has been proposed [10]. For a fixed OFDM bandwidth the larger the number of sub-carriers, the smaller the frequency spacing between sub-carriers. Therefore in systems with many sub-carriers, several adjacent sub-carriers can be clustered together and processed with the same set of weights. Allocation of cluster sizes can be equally or dynamically divided

depending on the channel and number of sub-carriers used [10].

1.3.2 IS-OFDM

The other strong interference cancelling scheme for OFDM systems present in literature is known as interference suppressing OFDM (IS-OFDM) [11] [12]. Here each data symbol is transmitted N times, where N is the number of sub-carriers used in the OFDM system. This effectively creates a redundancy in the transmitted signals which allows for narrow-band interference suppression. Narrow-band interference means that the interfering signals bandwidth is smaller than the desired users bandwidth.

Let the frequency domain transmitted data be represented by $[x_0, x_1, ..., x_{N-1}]$. Each transmitted symbol is replicated at each frequency bin. Hadamard encoding is applied to add orthogonality between replicated samples, which allows them to be distinguished and separated at the receiver. The transmitted data is arranged as follows,

$$\hat{\mathbf{X}} = \begin{bmatrix} x_0 & x_0 & \cdots & x_0 \\ x_1 & x_1 & \cdots & x_1 \\ \vdots & \vdots & \ddots & \vdots \\ x_{N-1} & x_{N-1} & \cdots & x_{N-1} \end{bmatrix} \tag{1.1}$$

where $\hat{\mathbf{X}}$ is an $N \times N$ matrix. Each column represents a frequency bin, and each row is subjected to an orthogonal Hardamard code. If the off diagonal terms were zero this system would be identical to a classical OFDM system. The data is then transformed into the time-domain using an inverse Fast Fourier Transform (IFFT). Finally the time-domain data is summed and transmitted. This system is equivalent to combining several OFDM systems in parallel in which the sub-carriers of each parallel system are orthogonal to each other.

Success of this method is based on the fact that narrow-band interfering signals are

used in the model. This means that some co-channel sub-carriers will be affected by the narrow-band interference, but the redundancy will ensure that most sub-carriers avoid any type of corruption. This effectively improves the performance of the system.

One of the drawbacks of this system is the extra processing required in the transmitter and receiver. OFDM already suffers from large one-way processing delays because of the necessary error control codes and interleaving procedures. Another disadvantage is that narrowband interference combined with the redundancy in transmitted signals results in an error floor in the bit error plots. This is shown in greater detail in Chapter 5.4.

1.4 Thesis Outline

This thesis is organized as follows. Chapter 2 discusses the fundamental concepts of an OFDM multi-carrier system. Its origins are investigated and traced to the current architecture that uses Fast Fourier Transform (FFT) techniques as part of the modulation and demodulation processes. A brief discussion on the advantages and disadvantages of OFDM compared to single carrier systems is then discussed.

Chapter 3 introduces the basic concepts of adaptive antenna arrays and beamforming techniques. The main focus in the first half of the chapter is formulating the steering vector representation based on equi-spaced uniform linear arrays. Finally the minimum mean squared error adaptive weight technique is investigated.

Chapter 4 presents a detailed study of OFDM systems combined with adaptive antenna arrays, and also introduces the frequency sub-carrier based (FSB) algorithm. Two methods to implement the FSB algorithm are established, the first method utilizes both the amplitude and phase of the zeros in the adapted beampattern at the center frequency to optimize weights for individual sub-carriers. The second method utilizes the phase only.

Chapter 5 examines the limits of the FSB algorithm using simulations of different

environments and system models. Detailed comparisons of bit error plots are investigated for each simulation. The first half of the chapter introduces models that the FSB algorithm shows successful improvement in system performance. The second half of the chapter investigates conditions where the FSB algorithm fails. Also reasons for the success and failure of the FSB algorithm are discussed.

Chapter 6 presents a summary of the key results and concludes the thesis. Also topics that can be investigated in future work are briefly discussed.

Chapter 2

Orthogonal Frequency Division Multiplexing

The fundamental concepts of orthogonal frequency division multiplexing (OFDM) are studied in this chapter. Evolution of the OFDM system model is traced from its original concepts introduced in the 1960s [19], to its present version which incorporates recent advances in technology [20]. Popularity and practicality of implementing OFDM systems in today's market is made possible because of advances in very large scale integrated circuits. Advantages and disadvantages of multi-carrier OFDM systems compared to single carrier systems are discussed.

2.1 Multi-Carrier Modulation

Multi-carrier modulation (MCM) systems such as frequency division multiplexing (FDM) and parallel data transmission systems, were first introduced in the 1960s [19]. These systems are attractive because they can achieve high data rates by exploiting large bandwidths. Practical mass implementation of FDM and parallel data transmission systems was impossible in those days because of limitations in technology and cost. Recent advances in digital signal processing (DSP) chips allow efficient, affordable and practical

implementation of MCM techniques. The main concept behind MCM techniques is to create a system with a high data rate which is composed of many lower rate data sub-carriers operating in parallel [4]. These lower rate sub-carriers are combined to create the overall transmit signal.

2.2 Fundamental concepts of OFDM

Classical MCM and parallel data systems do not allow spectral overlap in the frequency band. This is done in order to protect the system from inter-carrier (or inter-channel) interference (ICI). Instead, a small guard space is placed between adjacent sub-channels in the frequency band to isolate them for filtering purposes. This of course is an inefficient use of the bandwidth.

OFDM is a MCM technique which allows overlapping frequency sub-channels. Thereby creating a system that efficiently utilizes the available bandwidth. Spectral overlap in OFDM is made possible by making each data sub-carrier mathematically orthogonal to every other sub-carrier in the system. Two functions, $\varphi_n(t)$ and $\varphi_m(t)$ are said to be orthogonal over the interval $a < t < b$, if they satisfy the relation

$$\int_a^b \varphi_n(t)\varphi_m^*(t)dt = k_n\delta_{nm}, \tag{2.1}$$

where * represents the complex conjugate, k_n is a constant and $\delta_{nm} = 0, n \neq m$, and $\delta_{nm} = 1, n = m$. Figure 2.2 uses a sinc function to visually represent orthogonal spectral overlap in the frequency domain. Notice that the side-lobes of each sub-carrier pass through zero at the peak of every other sub-carrier, effectively making them orthogonal. This orthogonality allows easier recovery of data at the receiver and substantially increases bandwidth efficiency.

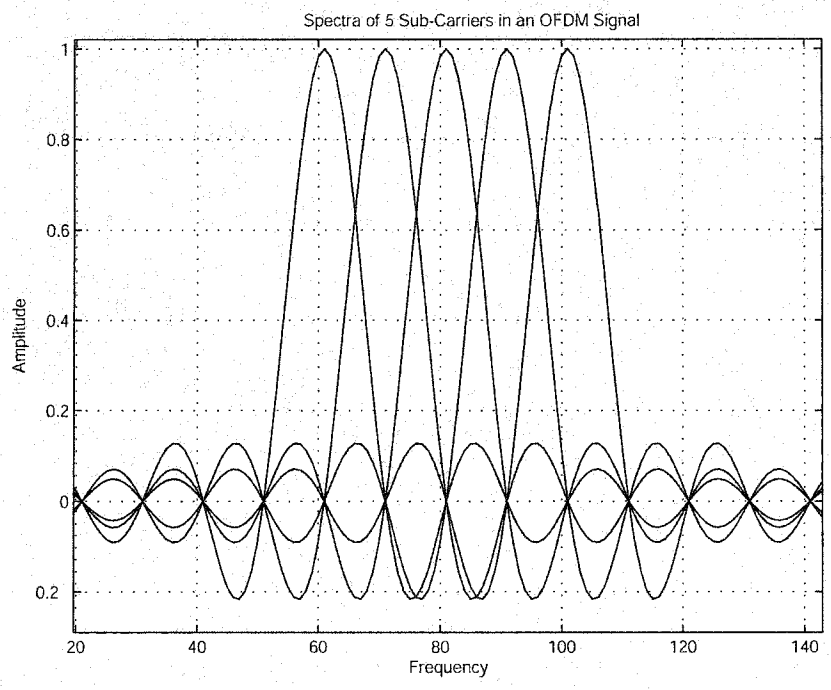

Figure 2.1: 5 sub-carriers exhibiting orthogonal spectral overlap

2.2.1 OFDM Transmitter

A block diagram of an OFDM transmitter is presented in Figure 2.2. Consider a system in which the desired symbol rate is $1/T$ symbols/sec, B is the number of bits/symbol for a given complex signal constellation and R is the code rate of the error encoder.

First a serial data bit stream is encoded with an error correcting code. The rate of the serial stream at the input of the encoder is B/RT bits/sec and the new data created at the output of the encoder has a bit rate of B/T bits/sec.

The encoded data is modulated to the desired complex signal constellation, using an M-point array with $B = \log_2 M$. Any M-array constellation could be used, but the most popular modulation techniques for OFDM systems tend to be phase shifting key (PSK) or quadrature amplitude modulation (QAM). After the data has been modulated to the appropriate constellation the symbol rate is given by $1/T$ symbols/sec.

Next diversity is added to the symbols with interleaving. Fading channels could effect

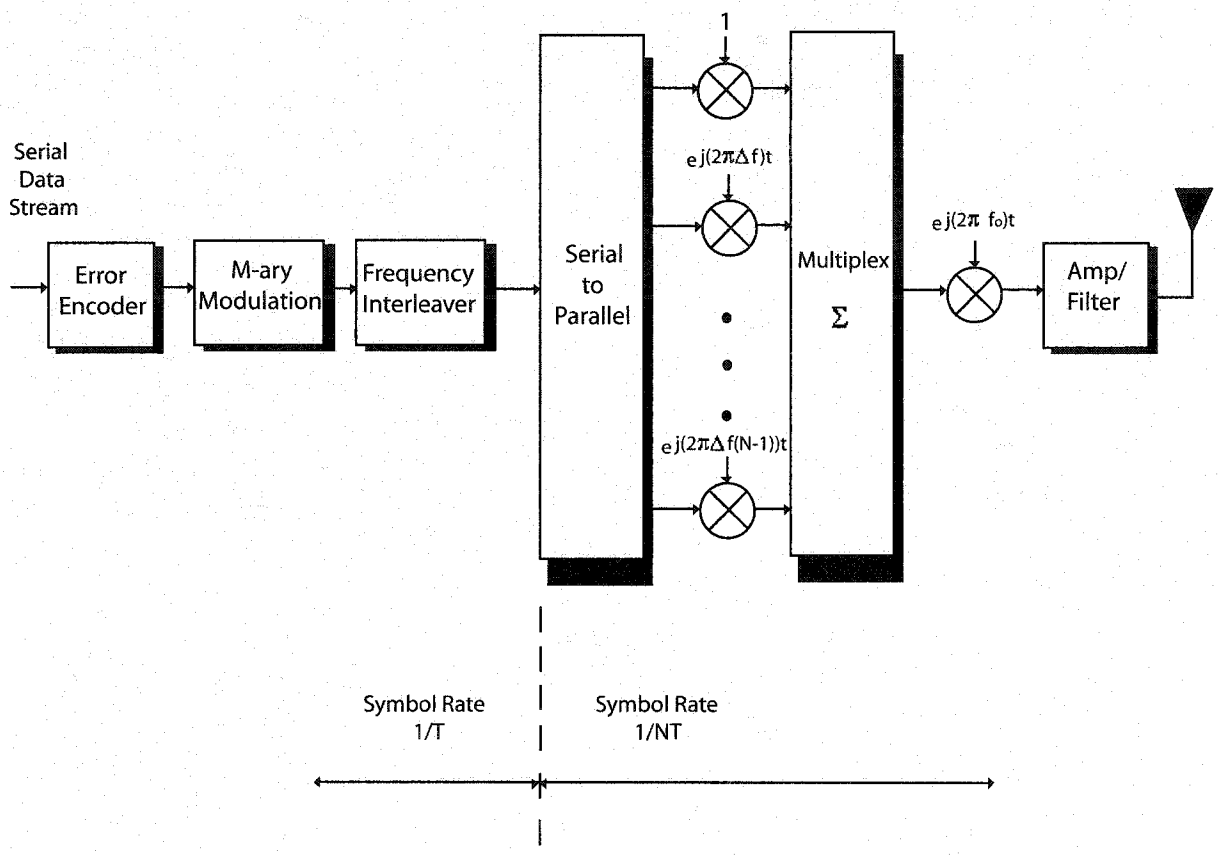

Figure 2.2: A block diagram of an OFDM transmitter

several consecutive sub-carriers rendering them useless. Interleaving is a process which permutates the data so that it reduces the effects of these burst errors. The use of error control codes and interleaving improves the performance of an OFDM system by making it more resistant to fading effects and generally making it more robust.

The data is then buffered and passed through a serial to parallel (S/P) converter. As mentioned before, the essence of MCM is to create a system with a high data rate which is composed of a several low data rate sub-carriers. Therefore it should be noted that the input to the S/P converter is N times faster then the output, where N represents the number of sub-carriers. Mathematically the symbol rate of each individual sub-carrier is given by $1/NT$ symbols/sec. Each sub-carrier modulates the data on a particular parallel branch using a complex sinusoidal carrier given by

$$\varphi_k(t) = e^{j(2\pi k\Delta f)t}, \tag{2.2}$$

where $k = 0, ...N-1$ and Δf is the frequency separation between adjacent sub-carriers.

The data modulated by the sub-carriers is then summed and up-converted to the desired passband frequency. Amplification and filtering of the signal are the final two steps in the transmission process. Mathematically the transmitted signal can be written in baseband as [3],

$$u(t) = \sum_{k=0}^{N-1} d(Ni+k)e^{j(2\pi k\Delta f)t}, \quad iNT < t \leq (i+1)NT, \tag{2.3}$$

where $d(Ni+k)$ represents the data symbol modulated by the k^{th} sub-carrier in the i^{th} data block and $u(t)$ represents the transmitted OFDM symbol.

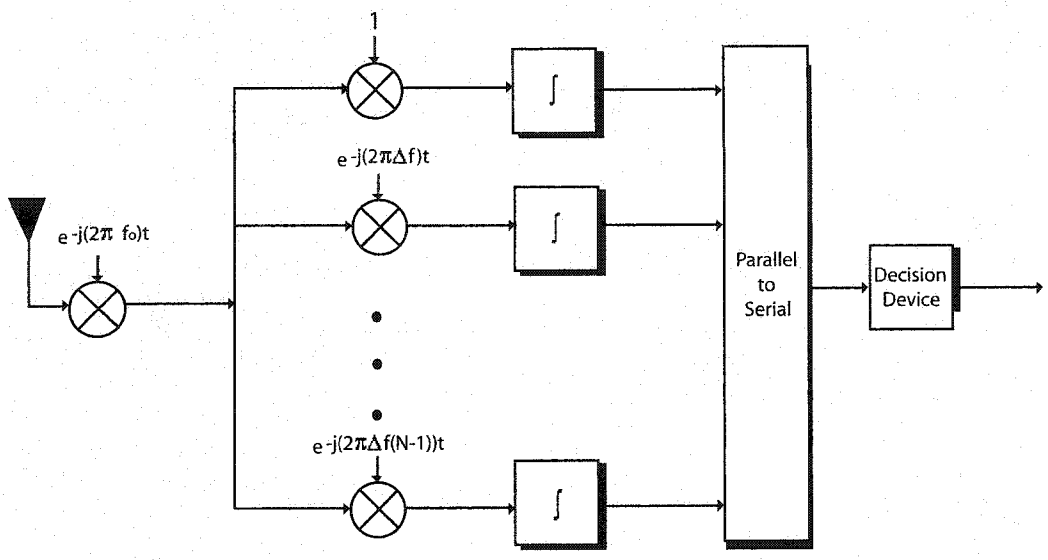

Figure 2.3: A block diagram of an OFDM receiver

2.2.2 OFDM Receiver

The received signal could be corrupted by many factors such as fading, noise, scattering, shadowing etc. This of course is dependent on the channel. A block diagram of an OFDM receiver is presented in Figure 2.3.

The received passband signal is down-converted to the baseband, then demodulated by each individual sub-carrier and integrated over a symbol interval. Due to the orthogonality of the system the data that originally modulated by each carrier in the transmitter can be recovered. Note that if the channel has a strong effect on the sub-carriers causing a frequency offset, the received symbols will not be orthogonal and will result in interference. Finally the data is converted back to a serial stream where a decision device is used to estimate the original transmitted data.

2.2.3 Frequency Separation Δf

Orthogonality between sub-carriers requires that Δf is chosen so that each sub-carrier satisfies the condition specified in Eqn. (2.1). In this system the orthognality between sub-carriers can be mathematically written as

$$\int_0^{NT} \varphi_k(t)\varphi_l^*(t)dt = \int_0^{NT} e^{j(2\pi k\Delta f)t}e^{-j(2\pi l\Delta f)t}dt = NT\delta_{kl}, \tag{2.4}$$

where k and $l = 0, 1, ..., N-1$. The formulation of the smallest non-zero value for Δf that satisfies the orthogonality condition in Eqn. (2.4) is [3],

$$\Delta f = \frac{1}{NT} \tag{2.5}$$

Any other choice of Δf would lead to inefficient use of the bandwidth and in some cases may result in interference.

2.3 OFDM using Fast Fourier Transforms

The multi-carrier OFDM system described in Figures 2.2 and 2.3 can be developed, but is unnecessarily complex and expensive, because it requires N precise frequency oscillators at the transmitter and receiver [1]. This also makes the system very rigid. If the frequencies are offset by even a small amount the orthogonality would be lost and could make the overall system unstable.

In 1971, Ebert and Weinstein found a solution to this problem which reduces the complexity of parallel systems significantly [20]. They use the Discrete Fourier Transform (DFT) to produce N orthogonal sub-carrier bins. An inverse DFT is used in the transmitter as part of the modulation process and a DFT is used in the receiver as part of the

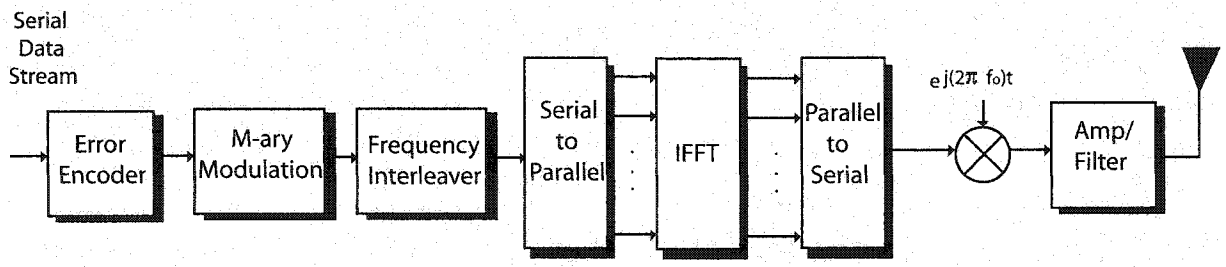

Figure 2.4: A block diagram of an OFDM transmitter using an IFFT

demodulation process. The FFT is an efficient implementation of DFT. Recent advances in DSP technology make FFT and IFFT chips practical and affordable to consumers.

Justification of incorporating IFFT and FFT as part of the OFDM scheme is presented next by showing its equivalence to the previously established model. The IFFT is expressed as

$$u[n] = \sum_{k=0}^{N-1} d(Ni+k)e^{\frac{j2\pi kn}{N}} \tag{2.6}$$

Sampling Eqn. (2.3) at a rate of $1/T$ samples/sec and using the minimum allowed frequency spacing between adjacent sub-carriers given in Eqn. (2.5), we can write

$$u(nT) = \sum_{k=0}^{N-1} d(Ni+k)e^{\frac{j2\pi nkT}{NT}} = \sum_{k=0}^{N-1} d(Ni+k)e^{\frac{j2\pi nk}{N}}, \tag{2.7}$$

which is the same as the IFFT shown in Eqn. (2.6).

Figure 2.4 presents a block diagram showing the transmitter of an OFDM system

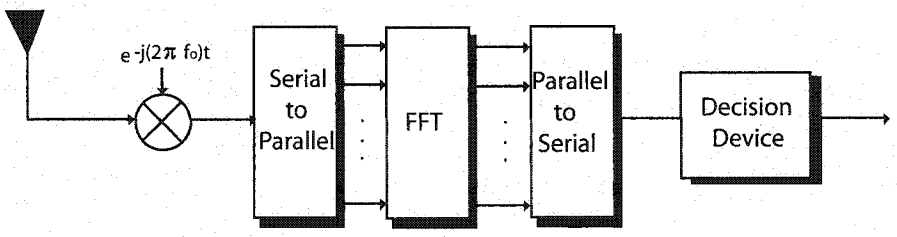

Figure 2.5: A block diagram of an OFDM receiver using a FFT

using IFFT techniques as part of the modulation process. The main difference between an OFDM transmitter using IFFT techniques to the one previously described is that when the serial stream is converted to a parallel stream, it is done with a symbol rate of $1/T$ symbols/sec. Every other step in the transmission process remains the same.

Figure 2.5 presents a block diagram showing the receiver of an OFDM system using FFT techniques as part of the de-modulation process. The received signal is first down-converted to baseband, where it is sampled at a rate of $1/T$ symbols/sec. A FFT is then implemented to de-modulate the data in each sub-carrier frequency bin back to frequency-domain. The parallel data at the output of the FFT is converted to a serial stream at a rate of $1/T$ symbols/sec. Finally a decision device is used to determine an estimated version of the original transmitted data.

2.4 Advantages and Disadvantages Of OFDM

In this section the OFDM multi-carrier model is compared to the single-carrier model. Advantages and disadvantages of both carrier schemes are considered and discussed in detail.

2.4.1 Advantages of OFDM versus Single carrier systems

Resistance to frequency selective fading

In an additive white gaussian noise (AWGN) channel, OFDM does not exhibit any real advantages when compared to any other carrier method. However, in a frequency selective fading channel, inter-symbol interference (ISI) occurs. A key result of OFDM is that the transmitted OFDM symbols may experience frequency selective fading but each data sub-carrier is only subjected to flat fading. This property allows for easier recovery of the data. No single carrier model can compete with how OFDM mitigates the effects of ISI.

To deal with ISI, a small guard time is concatenated to the end of the OFDM symbol. If the guard time is longer then the delay spread of the channel, the ISI is completely eliminated. The guard time should be chosen as cyclic extension of the OFDM symbol, since a timing synchronization problem may result in the receiver if zeros are placed in the guard period. The use of a guard time eliminates the need of adaptive equalizers, which are needed in the single-carrier case, therefore reducing the complexity of the system.

Increased Efficiency

Theoretically OFDM is the most spectrally efficient method because it allows spectral overlap. The increase in available bandwidth between an overlapping system and a non-overlapping system was shown in shown in Figure 2.1. Orthogonality of sub-carriers allows for this tight packing of data.

The use of IFFT and FFT in the modulation and de-modulation processes makes OFDM computationally efficient, since the FFT is an efficient form of the DFT, reducing the number of operations from $O(N^2)$ to $O(NlogN)$ [1]. This in turn reduces the complexity of the overall system.

2.4.2 Disadvantages of OFDM

High Peak to Average Power Ratio

In OFDM systems the summation of N sub-carriers may result in a large peak-to-average power ratio (PARP). By the central limit theorem, the modulation of N independent identically distributed random signals results in a transmitted signal that has a Gaussian probability density function (pdf) [3]. The Gaussian pdf is the root source of the PARP problem. The maximum possible average power increases when the number of sub-carriers (N) increases. Therefore RF power amplifiers with high PARPs are required. To prevent the transmitters amplifier from going into saturation or clipping the signal, the output power must be reduced N times below the saturation level to ensure that the system is operating in the linear region [21]. Doing so results in inefficient power amplifiers. The mitigation of the PARP problem has been studied in three categories [21]:

1) Signals with high PARP are excluded from transmission. This will lower the average power rate. Error control codes are relied upon to recover the lost data.

2) Different Scrambling codes are used on each OFDM symbol. The scrambled data with the smallest PARP is selected to be transmitted.

3) Signal distortion techniques are used, such as windowing, clipping and peak cancellation.

Sensitivity to Frequency Offset

As stated above, one of key advantages of OFDM systems is its ability to completely remove ISI with the use of a guard interval. This however is only true if perfect orthogonality between sub-carriers is assumed. In a real channel, ISI can be introduced if the

channel introduces a frequency offset. The interference is due to the loss of orthogonality between sub-carriers. A number of sources could cause the frequency offsets, such as Doppler shift, the use of a short guard time (i.e. less then the delay spread) and tone interference. The magnitude of the ISI introduced is related to the degree of frequency offset. If the frequency offset is large, then the system can become totally unreliable. Frequency synchronization is therefore very important for the stability of the overall system.

Dependence on ECC and Interleaving

In a multi-path environment, OFDM should not even be considered without using error control codes and interleaving. These two methods increase the proficiency of the system by lowering the bit error rate (BER) and make the system more robust when dealing with errors, but they also increase the processing delay. This delay may become a problem in fully duplexed systems that operate in real time such as wireless services [3]. This is not a factor in systems such as DAB and DVB.

2.5 Summary

In this chapter the fundamentals of OFDM systems were presented. First the classical OFDM system model was studied. Recent advances in technology allow for a more practical implementation of OFDM systems incorporating FFT/IFFT technology. The IFFT/FFT as part of the modulation and demodulation process in the OFDM system was then investigated. Finally advantages and disadvantages of the OFDM systems were discussed.

Chapter 3

Fundamentals of Adaptive Arrays and Beamforming

The basic concepts of adaptive antenna arrays and spatial processing (beamforming) techniques are explored in this chapter. Antenna arrays may be used in two forms. There are diversity techniques to combat small scale fading and beamforming techniques to suppress interference.

The chapter begins by presenting the basic concepts of smart antennas. Next assuming strong correlation between receive antenna elements, the formulation of the steering vector for uniform linear array geometries is devised. Finally classical adaptive beamforming techniques are presented.

3.1 Introduction

To improve the performance of future wireless systems the main goal consists of increasing the capacity of the system and reducing the probability of outage while maintaining spectral efficiency [8]. These goals can be accomplished by utilizing multiple element antenna arrays combined with spatial processing techniques. Which is why adaptive arrays will most likely be an integral factor in 4G mobile systems.

Interfering signals that reside in the same frequency band as the desired signal often originate from different spatial locations, resulting in distinctive angles of arrival (AOA) between received signals, thus giving them a unique spatial signature [21]. The spatial signature is exploited by adaptive array techniques such as beamforming to mitigate the interference in the system. A beampattern is a radiation pattern created around the antenna elements whose shape is determined by the weights of an array. Beamforming is the process of adapting the weights to create a beampattern which optimizes certain performance indices. In general, the goal is to place a mainlobe in the direction of the desired signal, while simultaneously placing nulls in the directions of interference. The performance indices that are optimized include, the mean squared error (MMSE) output energy (MOE) and signal to interference plus noise ratio (SINR).

Adaptive arrays can be contrived in two ways, either as a phased array or a diversity array [18] [22]. The performance of each method is highly dependent on the correlation between the receive antenna elements. A phased array exhibits the characteristics of having a strong correlation between antenna elements. If this is the case, beamforming is used to to combat the interference in the system. On the other hand, diversity arrays are most useful when fading is uncorrelated at the antenna elements. In practice the correlation is somewhere between the two extremes. In this thesis we focus on the use of phased arrays for interference suppression.

3.2 Uniform Linear Arrays on the Receive

For a given phased array the radiation pattern is determined by three factors, the geometry of the array, the feed currents and the radiation patterns produced by each element [21]. Typically the geometry of the array is made linear, circular or planar. In a linear array an ambiguity problem may exist, where the antenna array cannot distinguish between the desired signal from the interfering signals. This problem is present because

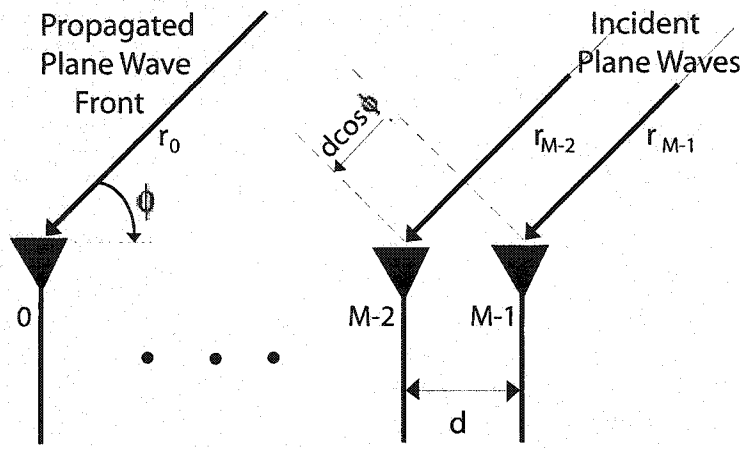

Figure 3.1: An M-element equispaced uniform linear array

of the sinusoidal nature of the steering vector defined later in this section. The feed currents and the radiation patterns are both dependent on the optimally determined weights at each element. Finally it should be noted that in this project it is assumed that each antenna element is isotropic, which means that each element equally radiates or receives energy in all directions. Isotropic elements are ideal elements which do not exist in practice, but the assumption is useful for research purposes.

The goal of this section is to formulate the mathematical representation of a steering for a uniform linear array (ULA). Figure 3.1 shows an M-element equispaced ULA, where ϕ represents the angle of arrival, d is the spacing between each element and r is the radial distance between the source of the signal and the receive array.

Consider the case where the signals are arriving from the far-field, i.e. the source of the signal originates far enough from the array that the radial distances of the arriving plane waves on each element can be considered parallel ($r_0 \parallel r_1 \ldots \parallel r_{M-1}$). The propagation delay between the elements can be determined as the wave propagates through the antenna. Using antenna element 0 as the reference element, it can be observed that the plane wave will arrive at element 1 Δt seconds after it arrives at element 0, where the propagation delay, Δt, is defined as

$$\Delta t = dcos(\phi)/c, \tag{3.1}$$

here c is the speed of light. Continuing with this logic and noting that each antenna element is equispaced, the received signal arrives at the next adjacent element Δt seconds after it arrives at the previous one, until the entire array is covered by the wave.

If it is assumed that the center frequency is much larger then the bandwidth of the signal, the narrowband signal model can be invoked. This model allows a small time delay to be represented as a phase shift, given by

$$e^{j(2\pi f \Delta t)} = e^{j(kdcos(\phi))}, \tag{3.2}$$

where the wave number, $k = 2\pi/\lambda$ and the wavelength of operation is represented by λ. Let us define a row vector that represents the received signal plane wave at each element, given by

$$\hat{\mathbf{y}}(t) = [y_0(t), y_2(t), ...y_{M-1}(t)]^T \tag{3.3}$$

where ^{T} represents the transpose and y_p represents the received signal at the p-th element. Using the phased shift given by the narrowband model in Eqn. (3.2), and remembering that each element receives a delayed version of the signal at the previous element we can re-write Eqn (3.3) in terms of the reference element, y_0. Mathematically this is written as

$$\hat{\mathbf{y}}(t) = [y_0(t), y_0(t)e^{j(kdcos(\phi))}, \ldots, y_0(t)e^{j((M-1)kdcos(\phi))}]^T \tag{3.4}$$

A length M phase response vector can be extracted from Eqn. (3.4) and is known as the steering vector. This is given by

$$\mathbf{s}(\phi) = [1, e^{j(kdcos(\phi))}, \ldots, e^{j((M-1)kdcos(\phi))}]^T \tag{3.5}$$

3.3 Beamforming

In this section we investigate the basic operation of a beamformer. A beamformer could be considered a spatial filter, since it exploits the spatial characteristics of the received signal to separate the desired signal from interfering signals. Beamforming increases the capacity of the system and reduces the probability of outage by mitigating the effects of interference, without increasing the allocated spectrum. The process of beamforming involves sampling and weighting the received signal based on a chosen performance criteria; the result is then summed at the output. An M-element narrowband beamformer is shown in Figure 3.2.

Consider a multi-user model in a additive white gaussian noise (AWGN) channel without fading. Given that K symbols are being transmitted by U users, the received signal can be written mathematically as

$$\mathbf{y}(t) = \sum_{i=0}^{U-1} \mathbf{s}(\phi_i)x_i(t) + \mathbf{n}(t) \tag{3.6}$$

where $x_i(t)$ is the transmitted symbols of the i-th user, ϕ_i is the AOA for the i-th user, $\mathbf{n}(t)$ is the complex noise and finally $\mathbf{s}(\phi)$ is the steering vector defined in Eqn. (3.5). Over K symbol intervals Eqn. (3.6) can be written in matrix form as

$$\mathbf{Y}(t) = \mathbf{S}(\phi)\mathbf{X}(t) + \mathbf{N}(t) \tag{3.7}$$

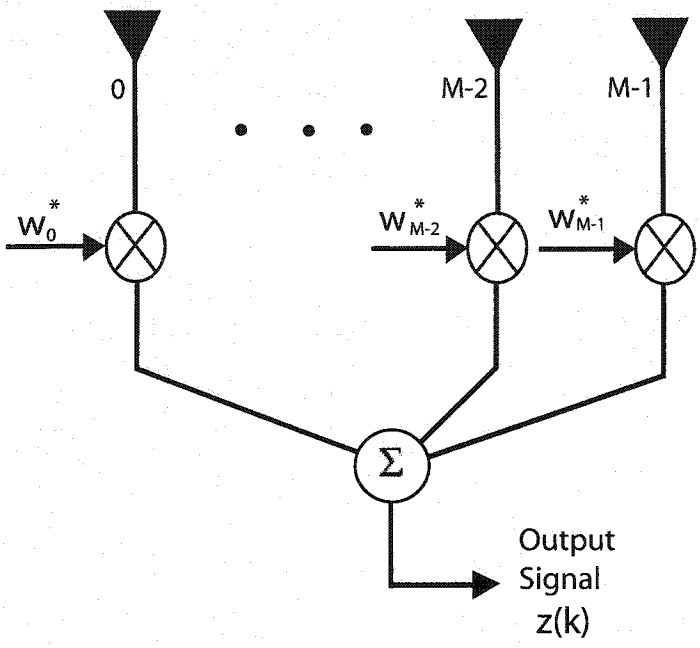

Figure 3.2: An M-element narrowband beamformer

where $\mathbf{S}(\phi)$ is the $M \times U$ matrix of steering vectors of the U users, $\mathbf{X}(t)$ is a $U \times K$ symbol transmission matrix, and $\mathbf{N}(t)$ is a $M \times K$ the AWGN matrix.

The received signal is processed at the adaptive array, where it is sampled, weighted and summed by the narrowband beamformer. This is mathematically shown by

$$z(k) = \sum_{i=0}^{M-1} w_i^*(k) y_i(k) = \mathbf{w}^H(k)\mathbf{Y}(k) \tag{3.8}$$

where $z(k)$ is the output of the beamforming process and $\mathbf{w}(k)$ is a $M \times 1$ weight matrix. Note that an M-element antenna array can only place $M-1$ nulls in the directions of interference. If there are greater than $M-1$ interfering signals an optimal beamforming technique adjusts the weights to minimize the overall output interference. Determining an optimal set of weights will be discussed in the next section.

3.4 Optimal Beamforming

As mentioned above the complex weights can be adapted to optimize certain performance indices. Several optimizing techniques exist, including iterative, non-iterative, blind and semi-blind techniques [8] [23]. Each method has its own advantages and disadvantages. But for purposes of this research, non-iterative techniques will be focused on. The three most common non-iterative beamforming techniques are minimum mean square error (MMSE), minimum output energy (MOE) and Maximum Signal-to-Interference Plus Noise Ratio. It can be shown that these are all theoretically equivalent.

3.4.1 Minimum Mean Square Error

One of the performance indices is to minimize the mean square error between the output of the narrowband beamformer $z(k)$, and a desired reference signal $d(k)$. This method minimizes the average power in the error signal [23]. Note that the receiver requires knowledge of the reference signal in the form of a training sequence which reduces the system throughput. The error signal we wish to minimize is given by

$$\mathbf{w}_{opt} = \arg\min_{w}(E\{|\mathbf{z}(k) - d(k)|^2\}) \tag{3.9}$$

$$\mathbf{w}_{opt} = \arg\min_{w}(E\{|\mathbf{w}^H(k)\mathbf{y}(k) - d(k)|^2\}) \tag{3.10}$$

$$\mathbf{w}_{opt} = \arg\min_{w}(\mathbf{w}^H\mathbf{R}\mathbf{w} - \mathbf{w}^H\mathbf{r}_{yd} - \mathbf{r}_{yd}^H\mathbf{w} + dd^*) \tag{3.11}$$

where $\mathbf{R} = E\{|\mathbf{y}\mathbf{y}^H|^2\}$ is the correlation matrix of the received data, and $\mathbf{r}_{yd} = E\{|\mathbf{y}\mathbf{d}^*|^2\}$ is the cross-correlation matrix between the received signal and reference signal. Here $E[\cdot]$ represents the ensemble average.

Taking the gradient of Eqn. (3.11) with respect to $\mathbf{w}^H$ and setting the result to zero minimizes the function and gives us the final result. The MMSE solution is written as

$$\mathbf{w} = \mathbf{R}^{-1}\mathbf{r}_{yd} \tag{3.12}$$

This result is also known as the Weiner filter in adaptive filter theory.

3.5 Direct Matrix Inversion

In practice it is computationally difficult or impossible to calculate the actual correlation matrix. Direct matrix inversion (DMI) is a process used to estimate the correlation matrix $\mathbf{R}$ with several snapshots of data. The estimated version of the received data correlation matrix and cross-correlation matrix are given by

$$\hat{\mathbf{R}} = \frac{1}{K}\sum_{k=1}^{K}\mathbf{y}_k\mathbf{y}_{k^H}, \tag{3.13}$$

$$\hat{\mathbf{r}}_{yd} = \frac{1}{K}\sum_{k=1}^{K}\mathbf{d}_k^*\mathbf{y}_k, \tag{3.14}$$

where K is the number of samples used to estimate the correlation matrix. The estimated weights are given by

$$\hat{\mathbf{w}} = \hat{\mathbf{R}}^{-1}\hat{\mathbf{r}}_{yd} \tag{3.15}$$

3.6 Summary

The main goals of this chapter were to establish the ULA, steering vectors and to introduce the MMSE non-iterative spatial processing technique. First adaptive antenna arrays were defined and studied. ULAs were then introduced, which led to the definition

of a steering vector. Finally the theoretical MMSE technique was introduced followed by the DMI, a practical implementation of MMSE.

Chapter 4

Frequency Sub-Carrier Based Weight Technique

This chapter presents a new method to extend adaptive weight techniques to mitigate strong co-channel interference in an OFDM system with adaptive antenna arrays. This frequency sub-carrier based (FSB) technique uses classical spatial processing methods to determine weights for the center frequency sub-carrier, and known frequency information to optimize the weights for individual sub-carriers. This results in a more robust and reliable OFDM system. Another contribution introduced in this chapter is a more precise technique to model steering vectors for broadband systems.

The chapter begins with a basic study of a multi-user OFDM system with adaptive arrays. The OFDM system is then extended to mitigate high-powered co-channel interference with the proposed FSB algorithm. Two methods to implement the FSB algorithm are presented. The first method uses the amplitude and phase of the zeros created from the optimal weights, and the second method uses the phase only.

4.1 Adaptive Beamforming for OFDM Systems

This section investigates the classical model of an OFDM system with adaptive antenna arrays. The combination of incorporating spatial processing techniques with the OFDM model produces an overall system with potentially high-data rates with interference cancelling capabilities. In 1999, Lee and Sollenberger first introduced how this system could be developed to mitigate co-channel interference [24]. Later in 2000, Kim, Lee and Cho improved on the original model by designing a new beamforming technique that utilizes the IFFT/FFT operation [25]. This section and chapter expands on the basic concepts presented by the improved model in [25].

An N-subcarrier, U-user block diagram of a basic OFDM system with an M-element receive antenna array is presented in Figure 4.1. Note that it was previously stated that OFDM should not be considered without error control codes or interleaving, but for purposes of this thesis these steps are unnecessary.

In the transmitter, N complex data symbols in the frequency-domain are modulated into the time-domain using the IFFT operation. After the data is transformed back into a serial stream it is up-converted to the passband and transmitted. The baseband time-domain OFDM symbol representation of the l-th sample of the block of data can be written as

$$y_l = \sum_{n=0}^{N-1} x_n e^{j2\pi(\frac{ln}{N})} \tag{4.1}$$

where x_n is the frequency-domain data symbol representation modulated by the n-th sub-carrier.

Over the N sub-carriers, Eqn. (4.1) can be written in vector form as

$$\mathbf{y} = \mathbf{F}^H \mathbf{x} \tag{4.2}$$

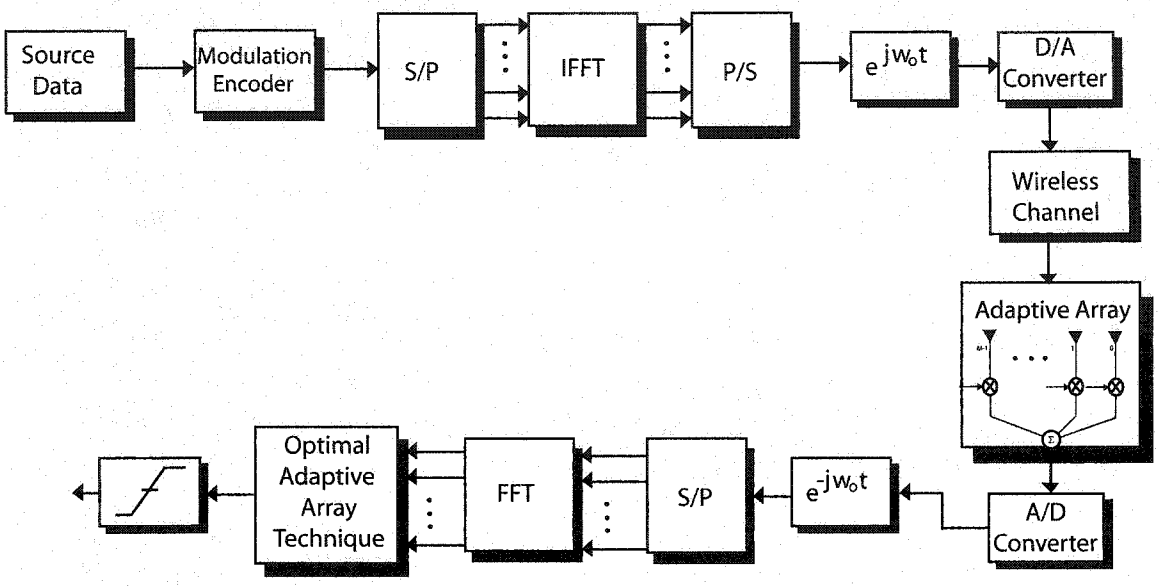

Figure 4.1: A block diagram of an OFDM system with a classical adaptive array

where,

$$\mathbf{y} = [y_0, y_1, ..., y_{N-1}]^T, \tag{4.3}$$

$$\mathbf{x} = [x_0, x_1, ..., x_{N-1}]^T, \tag{4.4}$$

$$\mathbf{F} = \begin{bmatrix} 1 & 1 & \cdots & 1 \\ 1 & e^{-j2\pi\frac{(1)(1)}{N}} & \cdots & e^{-j2\pi\frac{(1)(N-1)}{N}} \\ \vdots & \vdots & \ddots & \vdots \\ 1 & e^{-j2\pi\frac{(1)(N-1)}{N}} & \cdots & e^{-j2\pi\frac{(N-1)(N-1)}{N}} \end{bmatrix} \tag{4.5}$$

Here, $\mathbf{F}$ is the baseband matrix representation of the FFT operation. Note that the Hermitian of $\mathbf{F}$ results in the IFFT operation.

Since Fast Fourier techniques (IFFT/FFT) are implemented in the design of the modulation and demodulation processes of OFDM systems, the frequency information is

known to follow a cyclic pattern. Therefore the passband frequency bin information is given by

$$f_l = l(\Delta f) + f_o,\ l \in [-N/2, N/2 - 1], \tag{4.6}$$

where,

$$\Delta f = 1/NT_s. \tag{4.7}$$

Here, T_s is the OFDM symbol rate, f_l represents the passband frequency of the l^{th} sub-carrier and Δf is the minimum orthogonal frequency spacing between adjacent sub-carriers.

A broadband steering vector is now introduced to provide a more precise representation of the received signal at the antenna array. This model is developed for a single user. Given that the users DOA is located at angle ϕ_0 with respect the array, we define a vector $\mathbf{t}_l$,

$$\mathbf{t}_l = \mathbf{s}_l(\phi)x_l^T \tag{4.8}$$

where,

$$\mathbf{t}_l = [t_{0,l}\, t_{1,l}\, \ldots t_{M-1,l}]^T \tag{4.9}$$

$$\mathbf{s}_l(\phi) = \begin{bmatrix} 1 \\ e^{j2\pi\frac{f_l}{c}dcos(\phi_0)} \\ e^{j(2)2\pi\frac{f_l}{c}dcos(\phi_0)} \\ \vdots \\ e^{j(M-1)2\pi\frac{f_l}{c}dcos(\phi_0)} \end{bmatrix} \tag{4.10}$$

Here, d is the spacing between array elements, $l = 0, 1, ..., N-1$, $\mathbf{s}_l(\phi)$ is an $M \times 1$ steering vector for the l^{th} frequency, f_l, and x_l is l^{th} sample of transmitted frequency-domain data given in Eqn. (4.4). Equation (4.8) can be written as an $M \times N$ matrix, given by,

$$\mathbf{T} = \begin{bmatrix} x_0 & x_1 & \cdots & x_{N-1} \\ x_0 e^{j2\pi \frac{f_0}{c} dcos(\phi_0)} & x_1 e^{j2\pi \frac{f_1}{c} dcos(\phi_0)} & \cdots & x_{N-1} e^{j2\pi \frac{f_{N-1}}{c} dcos(\phi_0)} \\ x_0 e^{j(2)2\pi \frac{f_0}{c} dcos(\phi_0)} & x_1 e^{j(2)2\pi \frac{f_1}{c} dcos(\phi_0)} & \cdots & x_{N-1} e^{j(2)2\pi \frac{f_{N-1}}{c} dcos(\phi_0)} \\ \vdots & \vdots & \ddots & \vdots \\ x_0 e^{j(M-1)2\pi \frac{f_0}{c} dcos(\phi_0)} & x_1 e^{j(M-1)2\pi \frac{f_1}{c} dcos(\phi_0)} & ... & x_{N-1} e^{j(M-1)2\pi \frac{f_{N-1}}{c} dcos(\phi_0)} \end{bmatrix}$$

$\mathbf{T}$ allows us to define a more precise definition of the received signal. Assuming an additive white gaussian noise (AWGN) channel the received signal in the time-domain $\mathbf{V}$ can be written in matrix form as,

$$\mathbf{V} = \mathbf{T}\mathbf{F}^{\mathbf{H}} + \mathbf{B} \tag{4.11}$$

where,

$$\mathbf{V} = \begin{bmatrix} V_0^0 & V_1^0 & \cdots & V_{N-1}^0 \\ V_0^1 & V_1^1 & \cdots & V_{N-1}^1 \\ \vdots & \vdots & \ddots & \vdots \\ V_0^{M-1} & V_1^{M-1} & \cdots & V_{N-1}^{M-1} \end{bmatrix}, \tag{4.12}$$

and,

$$\mathbf{B} = \begin{bmatrix} B_0^0 & B_1^0 & \cdots & B_{N-1}^0 \\ B_0^1 & B_1^1 & \cdots & B_{N-1}^1 \\ \vdots & \vdots & \ddots & \vdots \\ B_0^{M-1} & B_1^{M-1} & \cdots & B_{N-1}^{M-1} \end{bmatrix}, \tag{4.13}$$

is an $M \times N$ AWGN matrix. So far we have defined the received signal for one user. The

model being studied has U users that share the same frequency channels. In practice, the interfering signals could be caused by delayed blocks of transmitted data, other transmitters or multi-path branches of the original signal. In a multi-user system Eqn. (4.11) and Eqn. (4.12) are reformulated for each users data and DOA ($\phi_u, u = 0, 1, \ldots U-1$ with respect to the array). The multi-user received signal can be represented as the sum of individual received matrices.

$$\mathbf{V} = \sum_{u=0}^{U-1} \mathbf{V}_U \tag{4.14}$$

The signal is then down-converted to the baseband and transformed back into the the frequency-domain with the FFT operation. The $M \times N$ frequency-domain received signal matrix is given by,

$$\mathbf{Q} = \mathbf{VF} \tag{4.15}$$

Adaptive processing techniques are used to process the received signal and determine the optimal weights $\mathbf{w}$, for each antenna element corresponding to the center frequency. These techniques optimize the desired signal based on a certain performance criteria and mitigate all other interfering signals. If the same weights are used at all frequencies the estimated interference free, but still distorted version of the receive signal represented by $\mathbf{r} = [r_o, r_1, \cdots, r_{N-1}]$, can be mathematically written as

$$\mathbf{r} = \mathbf{w}^H \mathbf{Q} \tag{4.16}$$

where,

$$\mathbf{w} = [w_0, w_1, \cdots, w_{M-1}]^T \tag{4.17}$$

The signal $\mathbf{r}$ is then fed through a decision device resulting in an estimate of the transmitted data.

4.2 Motivation

Since more devices are becoming wireless and because of limited frequency band allocations worldwide, strong co-channel interference caused by co-channel wireless LANs, jammers, and the near-far effect of ad-hoc networks will intensify in future OFDM systems [9]. Wireless LANs create strong interference if they are operating under the same frequency band in close proximity to each other. Therefore the probability of co-located LANs is dependent on the LANs popularity. Jammers are typically used in military type environments and in casinos, with the goal of producing enough interference to drown out the desired signal and degrade communications completely. Finally since ad-hoc networks do not operate under a centralized power source, a near-far effect could be caused by other ad-hoc devices in the vicinity. The issue of near-far effects is also important for cellular networks.

Researchers have proposed using wideband beamforming and IS-OFDM spatial processing schemes to mitigate strong co-channel interference in OFDM systems [9] [10] [11] [12]. The wideband beamforming approach is sub-optimal due to the resultant wandering of adaptive nulls as a function of the cluster frequencies. IS-OFDM schemes are sub-optimal due to the unnecessarily extensive redundancy in the transmitter. Both these methods were previously described in Chapter 1.

Classical broadband beamforming techniques are typically designed to optimize data for a single frequency. In broadband systems the center frequency is usually chosen as the desired frequency for optimization. Consider a 5-user, 5-element, OFDM system using the received signal representation given in Eqn. (4.11) and Eqn. (4.14). The power of

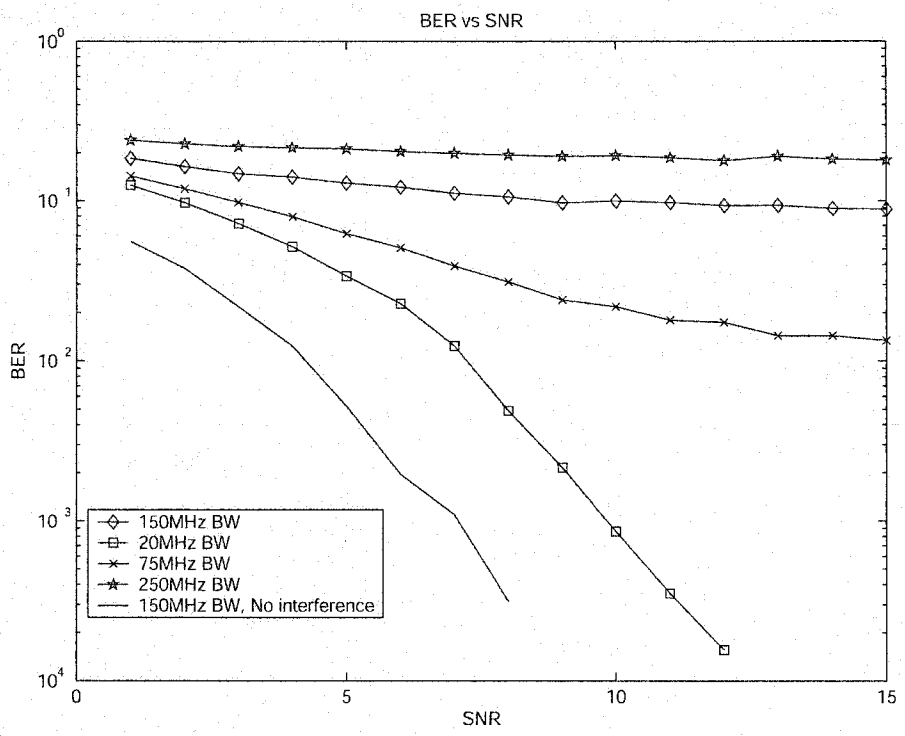

Figure 4.2: Divergence of the MMSE for broadband systems.

the desired signal is 12dB below the four interfering signals. Figure 4.2 investigates the divergence of the MMSE bit error rate as the bandwidth of the system is increased. A single set of weights produced for the center frequency does not provide accurate interference cancellation for each sub-carrier across the spectrum. This results in a significant increase in bit error rate for systems with larger bandwidths. The larger the bandwidth for the multi-carrier system the larger inaccuracy of the center frequency weights.

One of the main motivations behind this thesis is that the known frequency information given by the IFFT/FFT is not being exploited. We next introduce the FSB adaptive weight technique, which is designed to take advantage of the known frequency information to optimize the center frequency weights for each sub-carrier.

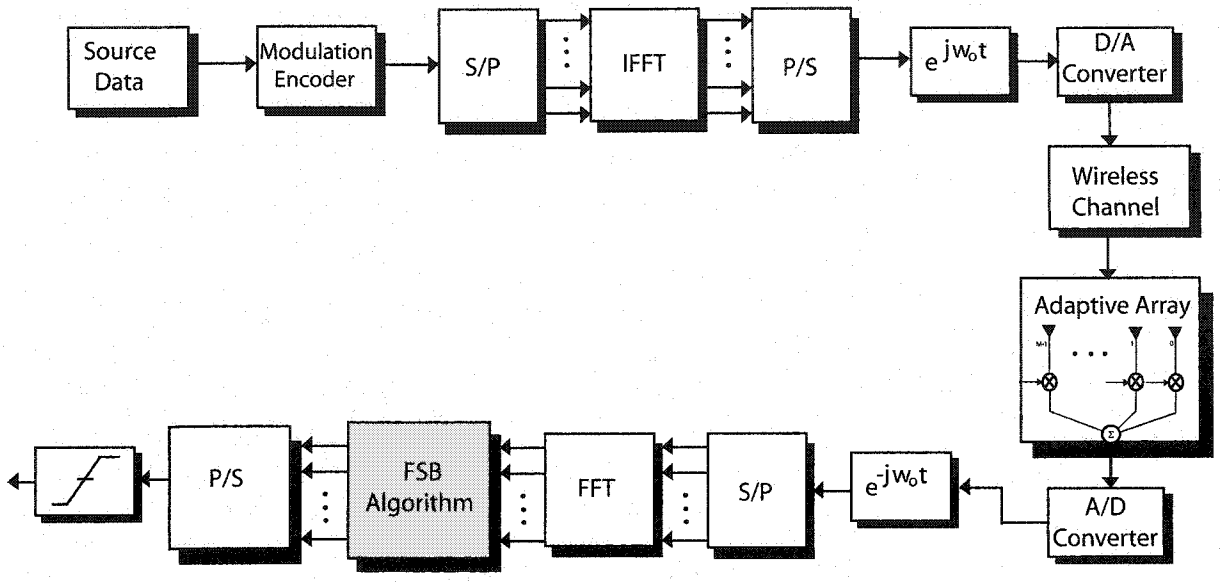

Figure 4.3: A block diagram of an OFDM system with the FSB algorithm

4.3 Frequency Sub-Carrier Based Interference Cancellation - Method I

In this section a new effective co-channel interference suppressing algorithm is introduced. Using known frequency bin information and the optimal weights of one narrowband beamformer, individual weights for each sub-carrier are constructed. This frequency sub-carrier based technique is significantly less complex when compared to the wideband beamformer and IS-OFDM.

Figure 4.3 shows the FSB block integrated into an U-user, N-subcarrier block diagram of an OFDM system with an M-element receive antenna. The received signal is processed in the frequency-domain, where a beamforming technique is implemented to determine optimal weights at the center frequency of the broadband signal. The first step of the FSB algorithm is to use a classical narrowband optimal weight technique to determine these center frequency weights. At this stage the FSB algorithm is implemented to determine the weights for specific sub-carriers using the frequency information given in Eqn. (4.6).

The success of the FSB technique is based on securing null locations for every sub-carrier at the needed angle of arrival. The FSB technique begins by recognizing that the optimal beamforming technique creates nulls in the interference directions. The physical location of these nulls should not change with frequency.

To determine a new set of weights for each individual sub-carrier, the FSB algorithm constructs a polynomial using the optimal weights of the center sub-carrier as coefficients. This is given by

$$p(z) = w_0 + w_1 z + ... + w_{M-1} z^{M-1} \tag{4.18}$$

where,

$$z = e^{j2\pi \frac{f_o}{c} d cos(\phi)} \tag{4.19}$$

This polynomial $p(z)$ represents the behavior of the optimal weights for all angles of arrival. Plotting the magnitude of $p(z)$ versus azimuth angles represents the beampattern graph, which gives a visual representation of null locations. This polynomial representation is valid because of the linear planar front in the definition of the steering vector. The zeros of Eqn. (4.18) represent the directions of interference (DOI) determined by the adaptive process. These zeros are found by taking the roots of the polynomial. Mathematically, this is given as

$$p(z) = (z - z_{0,o})(z - z_{1,o})...(z - z_{M-2,o}) \tag{4.20}$$

Here $z_{q,o}$ represents the zeros associated with the q-th null at the center frequency, where $q = 0, 1, ..., M-2$. The DOI for each null can now be determined by re-arranging Eqn. (4.19), giving

$$\cos(\hat{\phi}_q) = \frac{c}{j2\pi f_o d} \ln(z_{q,o}), \tag{4.21}$$

Physically the interference directions are independent of frequency. A root polynomial similar to Eqn. (4.20) can therefore be determined for individual sub-carriers using new zeros. The new polynomial for the l^{th} subcarrier is given by

$$p_l(z) = (z - z_{0,l})(z - z_{1,l})...(z - z_{M-2,l}) \tag{4.22}$$

where the new zeros are represented by

$$z_{q,l} = e^{j2\pi \frac{f_l}{c} d\cos(\hat{\phi}_q)}. \tag{4.23}$$

Here $z_{q,l}$ represents the zeros for the l-th sub-carrier and f_l is the frequency bin values given in Eqn. (4.6). The polynomial coefficients are determined from the roots. The coefficients of the new polynomials are the weights at each frequency for individual sub-carriers. The weight matrix is given by

$$\mathbf{W} = \begin{bmatrix} w_0^0 & w_1^0 & \cdots & w_{N-1}^0 \\ w_0^1 & w_1^1 & \cdots & w_{N-1}^1 \\ \vdots & \vdots & \ddots & \vdots \\ w_0^{M-1} & w_1^{M-1} & \cdots & w_{N-1}^{M-1} \end{bmatrix} \tag{4.24}$$

Here the l-th row represents the weights for the l-th sub-carrier of the block of data. Finally the Hermitian of the weights is multiplied by the received signal, resulting in a desired signal with interference suppressed. This is given by

$$\tilde{\mathbf{r}} = \mathtt{diag}(\mathbf{W}^H\mathbf{Q}) \tag{4.25}$$

The frequency-domain representation of the estimated signal after it is fed through a decision device can then be determined.

4.3.1 Summary of the FSB Algorithm: Method I

The FSB alogithm is a adaptive beamforming extension that makes OFDM systems more robust in high-powered co-channel interference environments. In general the FSB algorithm could be summarized in seven steps. These steps are:

1) Obtain weights for the center frequency using classical spatial processing techniques.
2) Create the $p(z)$ polynomial using the weights from step one as coefficients.
3) Find the zeros of $p(z)$.
4) Treat these zeros as corresponding to the directions of the interference.
5) Create new values of roots for individual sub-carriers by using the frequency bin information.
6) Convert the new values for the roots back to the weights polynomial.
7) The coefficients of the new weight polynomials are the weights for individual sub-carriers.

The FSB algorithm described in this section uses both amplitude and phase of the center frequency's zeros to construct new zeros for individual sub-carriers. Next a slightly more efficient version of the FSB algorithm is presented.

4.4 Frequency Sub-Carrier Based Interference Cancellation - Method II

Another approach to implement the FSB algorithm is introduced in this section. The motivation for this approach comes from the fact that theoretically the information regarding the DOI is in the phase of the nulls, not the magnitude. By focusing on the complex portion of the phase given by the center frequency zero values, identical results as method I can be achieved with fewer calculations. Once again the FSB algorithm is initiated after the the optimal weights are determined for the center frequency. Method II of the FSB algorithm begins the same as method I. The classically determined optimal weights are used as coefficients of the $p(z)$ polynomial, repeated here for convenience

$$p(z) = w_0 + w_1 z + ... + w_{M-1} z^{M-1} \tag{4.26}$$

where,

$$z = e^{j2\pi \frac{f_o}{c} dcos(\phi)} \tag{4.27}$$

Again the zeros of $p(z)$ are found, and are given by

$$p(z) = (z - z_{0,o})(z - z_{1,o})...(z - z_{M-2,o}) \tag{4.28}$$

Since the information regarding the DOI is in the phase only, we can estimate the DOI as

$$\ln(z_{k,o}) = z_k^{(1)} + j z_k^{(2)} \tag{4.29}$$

$$\cos(\tilde{\phi}_k) = \frac{c}{2\pi f_o d}(z_k^{(2)}) \tag{4.30}$$

Equation (4.30) also indicates that the phase term, $z_k^{(2)}$, is directly proportional to frequency. The complex nulls associated in the other subcarrier frequencies can now be determined for each sub-carrier. The new values for the roots of the l^{th} sub-carrier are given by

$$z_l^k = e^{z_k^{(1)} + j\frac{f_l}{f_o} z_k^{(2)}} \tag{4.31}$$

Here the l^{th} sub-carrier frequency given in Eqn. (4.6) is input for f_l, effectively creating new zeros specific to each sub-carrier. The weights for the sub-channels are the coefficients of the polynomial.

$$p_l(z) = (z - z_{0,l})(z - z_{1,l}) \ldots (z - z_{M-2,l}). \tag{4.32}$$

The remaining steps of the FSB algorithm remain the same as before. A matrix of weights $\mathbf{W}$, is constructed for all sub-carriers. After the desired signal is separated from interfering signals, it is fed through a decision device, resulting in an estimated version of the original data.

4.4.1 Summary of the FSB Algorithm Method II

Method II of the FSB algorithm can be summarized in six steps:

1) Obtain weights for the center frequency using classical spatial processing techniques.

2) Create the polynomial, $p(z)$ using these weights as coefficients.

3) Find the zeros of $p(z)$.

4) Use only the imaginary part of the phase given by z_2 to determine new zeros for individual sub-carriers.

5) Convert the new zeros back to a polynomial of weights.

6) The coefficients of the new weight polynomials are the weights for individual sub-carriers.

It should be noted that researchers have suggested a similar approach for downlink beamforming using uplink weights [26].

4.5 Summary

This chapter has explored OFDM systems combined with adaptive antenna arrays. Together this combination allows the OFDM model to mitigate co-channel interference to increase capacity, decrease probability of outage and allow a high data rate.

The second portion of this chapter focused on the new FSB techniques. The FSB algorithm is an innovative procedure compared to existing methods of mitigating high-powered co-channel interference. Basically the FSB algorithm is an extension to existing optimal weight techniques. This chapter described the new algorithm in two methods. The first method used the amplitude and phase of the center frequency zeros and the second method used only the phase.

Chapter 5

Numerical Results

This chapter examines the capabilities of the FSB algorithm in a virtual simulation environment. The FSB algorithm is exposed to different system parameters and channel models to discern how it behaves under different and stressful conditions. Performance is measured by the improvement of the BER versus SNR when comparing the FSB adaptive weight technique with adaptive weight techniques of [23]. Each section of this chapter begins with a short description of the system model, a table of parameters and the type of channel used. Then discussions of simulated results are presented.

The chapter begins with system models and channels which show successful improvement of the bit error plots for the FSB algorithm. Reasons for the improvement are then studied. Finally the remaining portion of the chapter examines system models where the FSB algorithm fails.

5.1 AWGN Channels Without Fading

The first simulation uses an AWGN channel without any fading, i.e. a line of sight channel is studied. The transmitted signal for this model was given in Eqn. (4.1). Assuming that the received signal is totally correlated between receive antenna elements, therefore the received signal can be modelled with the broadband steering vector origi-

nally presented in Eqn. (4.10). This entire system model was studied in detail in the last chapter.

The object of this section is to illustrate the interference suppressing capabilities of the FSB algorithm for different interference levels. The main parameters used for this example are given in Table 5.1.

Table 5.1: System Parameters

Parameters	**Actual Values Used**
Total OFDM bandwidth	150 MHz
Center frequency f_o	5 GHz
Number of Users, U	5
Number of sub-carriers, N	256
Number receive antenna elements, M	5
Strength of Interfering Users	4×0 dB, 4×6 dB, 4×12 dB, 4×20 dB
Direction of arrivals for U-users	$50^o, 70^o, 90^o, 110^o, 130^o$
Data Modulation	BPSK
Antenna spacing between elements, d	$\lambda/2$

The interfering wideband signals are assumed to reside in the same frequency channels as the desired signal. In this example, all the interfering users share the same power level. The interference power was varied from 0dB to 20dB greater then the desired user, following the values given in Table 5.1. The MMSE algorithm is the chosen classical narrowband beamforming scheme to which results are compared to [23]. Note that the MMSE is implemented using direct matrix inversion for all simulations in this chapter. K=256 samples were used to estimate the cross-correlation matrix, as well as the received data correlation matrix.

Figures 5.1 to 5.4 show the BER versus SNR using the MMSE technique and the

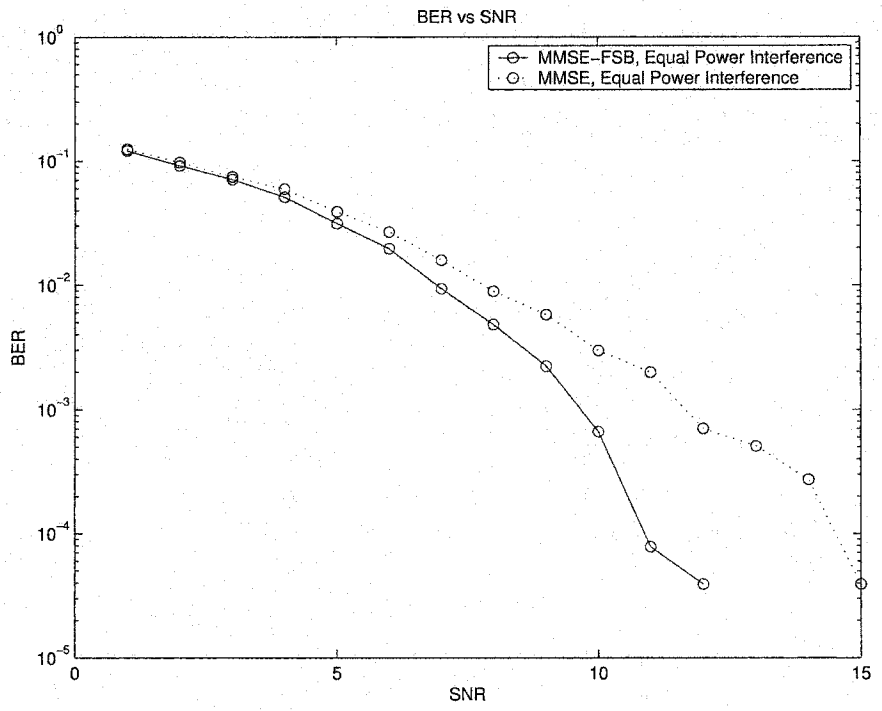

Figure 5.1: BER vs SNR, 4x0dB interfering users

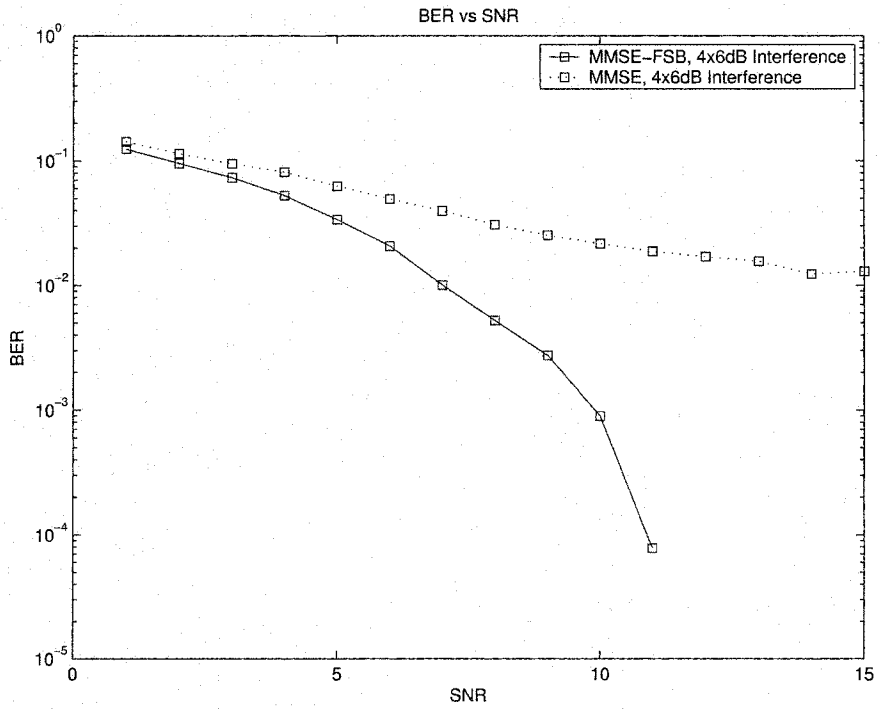

Figure 5.2: BER vs SNR, 4x6dB interfering users

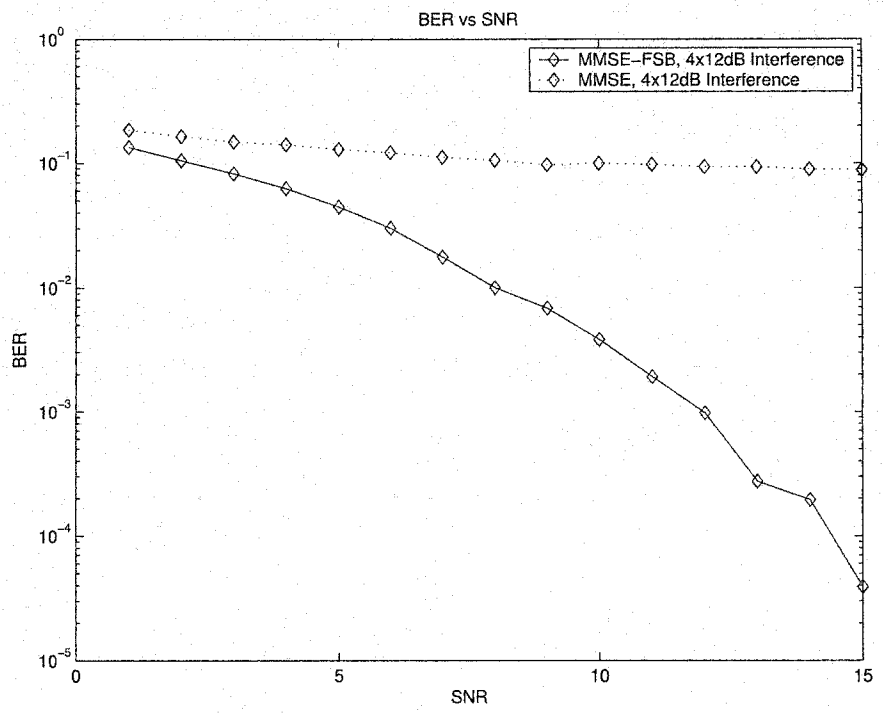

Figure 5.3: BER vs SNR, 4x12dB interfering users and

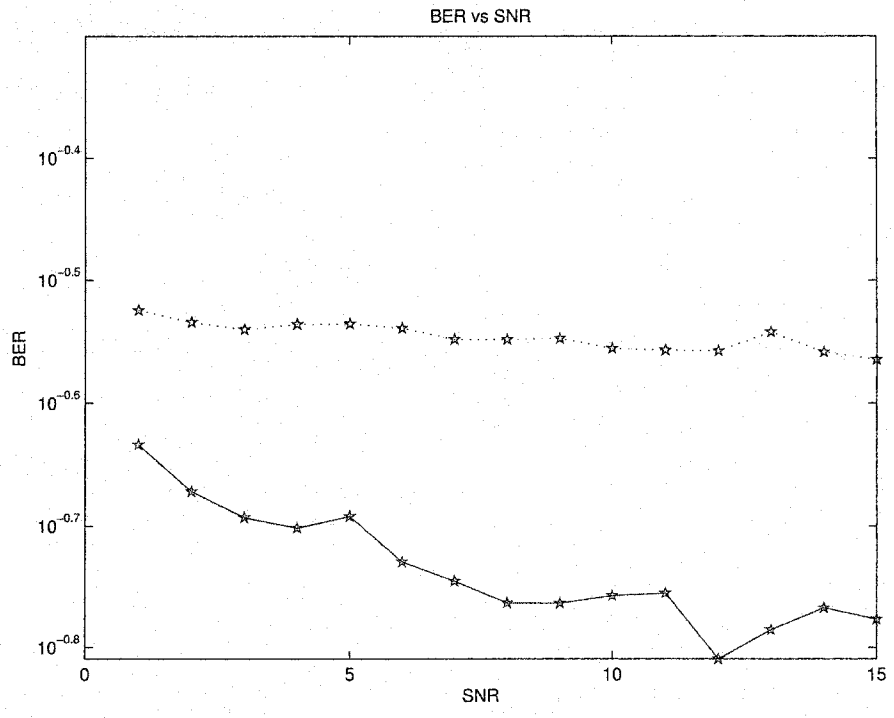

Figure 5.4: BER vs SNR, 4x20dB interfering users

MMSE-FSB technique for different levels of co-channel interference. Consider Figure 5.1, where the power level of the four interfering signals is equal to the desired users power. Focusing at a BER of 10^{-3}, the MMSE-FSB algorithm shows approximately a 2dB SNR improvement over the MMSE technique. However, clearly with no interference, the use of the same weights at all frequencies yields good results. Figure 5.2 and Figure 5.3, show a gradual divergence in the performance of the MMSE algorithm as higher levels of interference are introduced. Finally examining Figure 5.4 where the power level of the interfering signals is fixed at 20dB, although the MMSE-FSB shows a larger resistance to interference, both methods diverge considerably. Overall, these figures show that the MMSE-FSB algorithm performance remains stable at lower strength interference levels, and then gradually diverges, while the classical MMSE algorithm's performance diverges considerably for all increasing interference levels. The performance improvement is based on null deviation in an interference limited environment. This will be studied thoroughly in section 5.5.

5.1.1 Effect of different OFDM Bandwidths

This section investigates the effects of changing the OFDM bandwidth for the above system. The same number of sub-carriers are used for every simulation, meaning that the frequency spacing between adjacent sub-carriers will be smaller when a smaller bandwidth is used. This increases the bandwidth efficiency of the system but also leaves it more vulnerable to frequency offsets such as Doppler spread [4]. Note that Doppler spread is not considered in this example. Simulations in this section use the parameters described in Table 5.1, with the following changes, the bandwidths used for each simulation iteration are 20MHz, 75MHz, 150MHz, and 250MHz and the power of the four interfering users is fixed at 12dB.

Figures 5.5 to 5.8 show the effect that changing the OFDM bandwidth has on the bit error rate. Observing the 20MHz bandwidth system simulated in Figure 5.5, at a BER

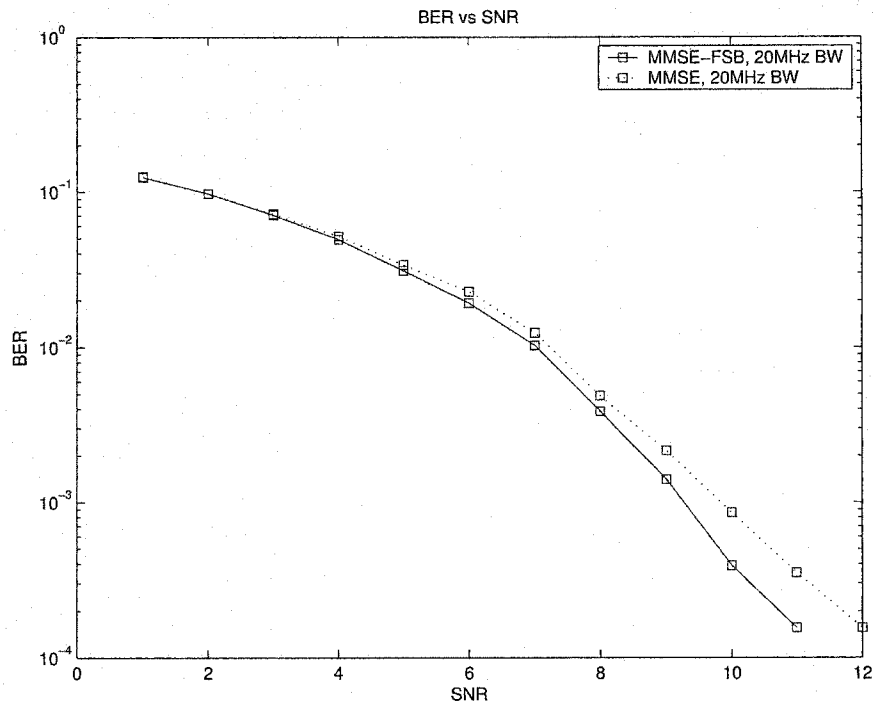

Figure 5.5: BER vs SNR, 20MHz bandwidth

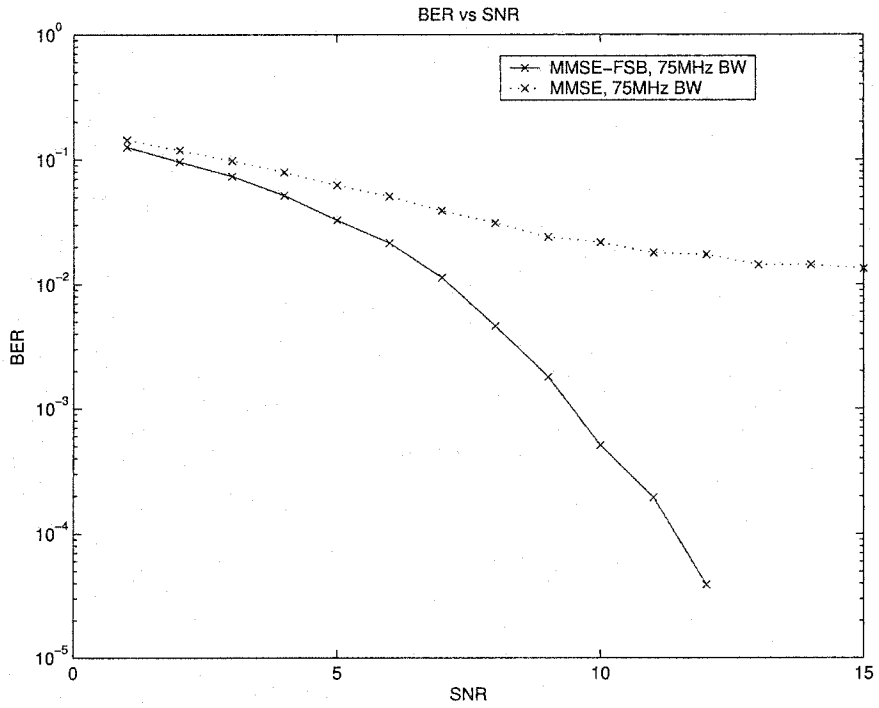

Figure 5.6: BER vs SNR, 75MHz bandwidth

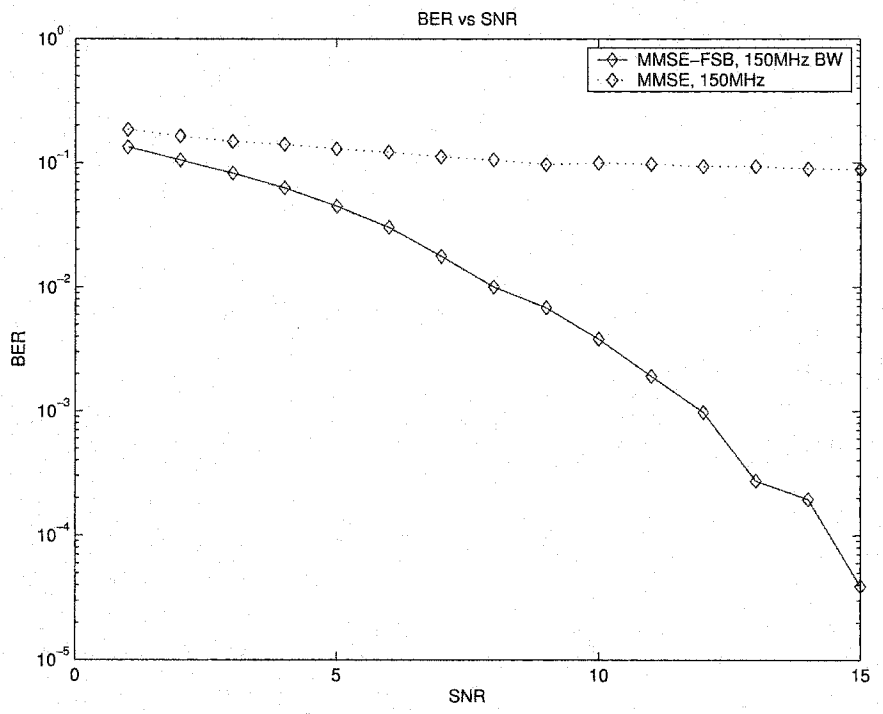

Figure 5.7: BER vs SNR, 150MHz bandwidth

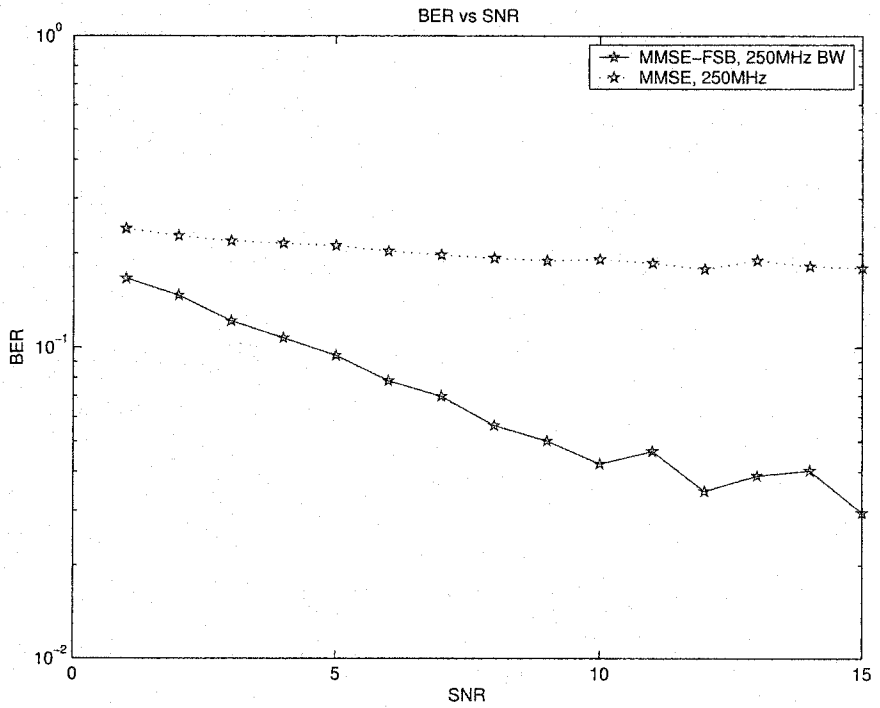

Figure 5.8: BER vs SNR, 250MHz bandwidth

of 10^{-3} MMSE-FSB shows approximately 0.5dB performance improvement, compared to MMSE. Figure 5.6 shows how fast the MMSE performance diverges when the bandwidth is increased. Further, when the bandwidth is increased to 150MHz and 250MHz shown in Figure 5.7 and Figure 5.8, respectively, the MMSE-FSB techniques performance begins to digress. Therefore simulation results show that the FSB algorithm significantly improves the performance of the system for larger OFDM bandwidths compared to the classical MMSE weight technique. As the bandwidth is increased, MMSE's performance diverges because a larger deviation in the wideband steering vector is present between the lowest and highest frequency of the broadband system, this results in larger null deviation which will be considered in section 5.5.

5.1.2 Varying the number of sub-carriers

Next we investigate the effect that changing the number of sub-carriers has on the BER performance. Generally the number of sub-carriers used in the wideband OFDM system determines the [1]:

1) Frequency stability, due to the sensitivity of frequency offset.
2) Delay sensitivity required, increasing the number of sub-carriers increases the symbol duration.
3) Maximum delay spread that can be tolerated.
4) The number of users the bandwidth can be spread over, for example the maximum theoretical bound is one user per carrier.

Figure 5.9 shows the BER versus SNR plot for a 150MHz bandwidth, AWGN OFDM system using 32, 64, 128 and 256 sub-carriers. Other parameters used in this simulation are described in Table 5.1. Observations indicate that the MMSE technique's performance slightly deteriorates as the number of sub-carriers increases, while the performance

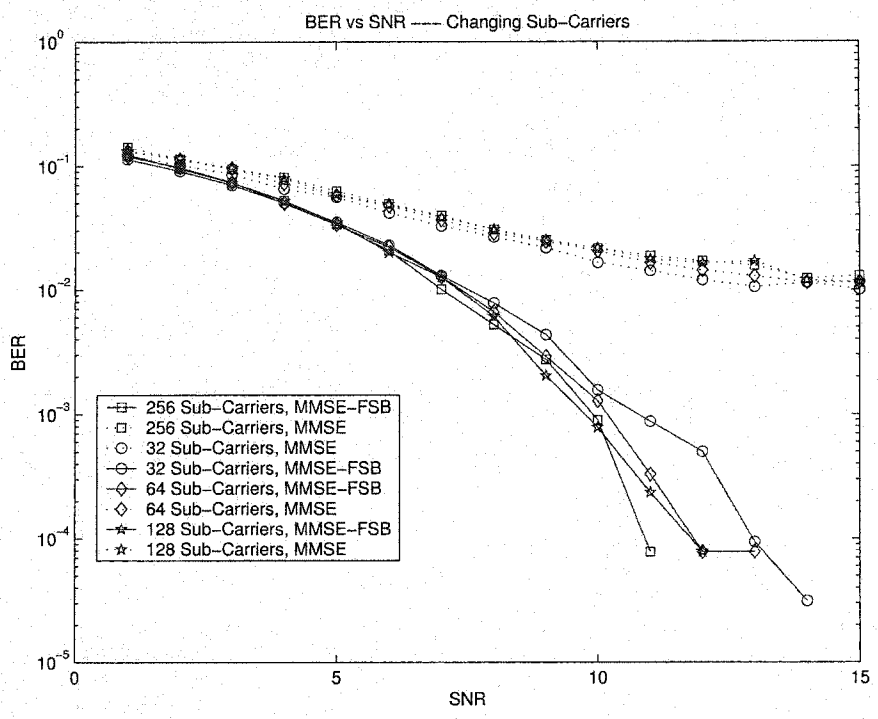

Figure 5.9: BER vs SNR, effect of changing the number of sub-carriers

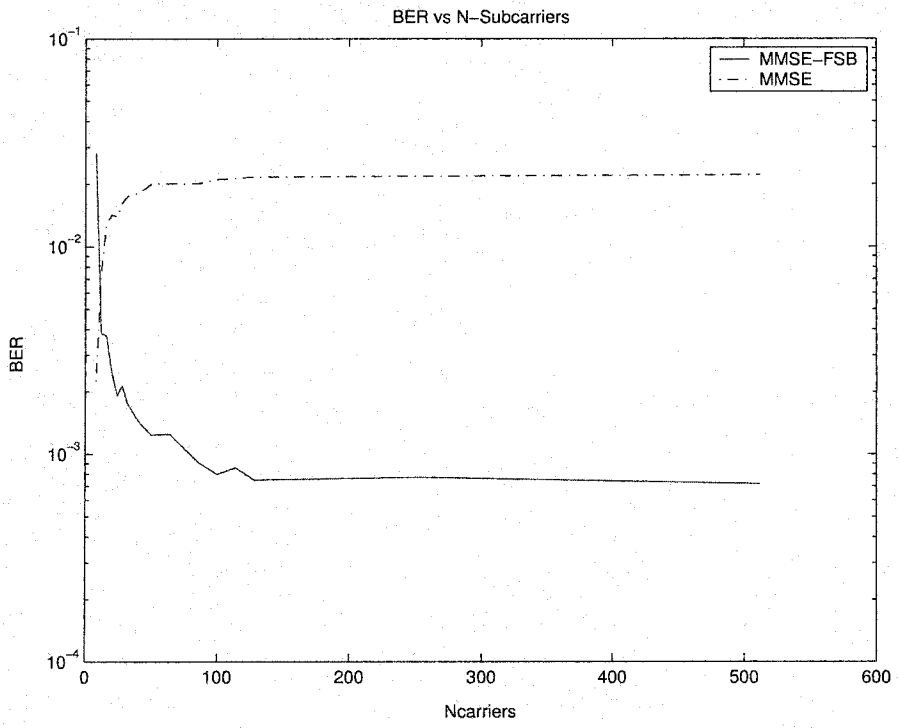

Figure 5.10: BER vs Number of sub-carriers for SNR=10dB

of the MMSE-FSB technique improves for a larger number of sub-carriers.

To confirm these observations, the BER versus the number of sub-carriers is plotted in Figure 5.10. The SNR is fixed to 10dB and the interference power is fixed at 4×6dB higher then the desired user. The figure confirms previous observations.

5.1.3 Special Case - IEEE 802.11a

In the final simulation using the AWGN channel, the behavior of the FSB algorithm using the parameter set listed in IEEE 802.11a standard is examined. The IEEE 802.11a is a wireless LAN standard which defines a set of requirements for the physical layer and medium access control layer [1]. In this simulation the model does not follow the exact stringent set of parameters listed by the standard. For example, convolutional codes, encryption and pilot symbols were not implemented. However basic parameters such as bandwidth, element spacing and number of sub-carriers were designed to standard. Specifically the parameters used in this simulation are listed in Table 5.2. The goal of this section is to confirm the results in the previous sections using different parameters.

The bit error plots using the standard 802.11a parameters are shown in Figure 5.11. The MMSE-FSB algorithm shows no improvement over the MMSE algorithm when the four interfering signals power is equal to the desired signal. In the next simulation, the power of the four interfering users is set to 20dB above the desired user. The MMSE performance diverges considerably, while the MMSE-FSB performance remains relatively steady. At a BER of 10^{-3} the MMSE-FSB shows approximately 3dB improvement. Like in previous simulations, as stronger interfering signals are introduced, the MMSE-FSB algorithm retains a relatively stable system performance, while the MMSE algorithm's performance begins to diverge. Larger interfering powers were need to show some performance improvement of the FSB algorithm because a 20MHz bandwidth is used. Therefore the MMSE and MMSE-FSB placed relatively similar nulls with small deviation between the first and last sub-carrier. Again this is discussed in greater detail in section 5.5.

Table 5.2: IEEE 802.11 a system Parameters

Parameters	**Actual Values Used**
Total OFDM bandwidth	20 MHz
Center frequency f_o	5 GHz
Element spacing Δf	312.5 KHz
Number of Users, U	5
Number of sub-carriers, N	52
Number receive antenna elements, M	5
Strength of Interfering Users per Iteration	$4\times$ Equal Power, 4×20 dB
Direction of arrivals for U-users	$50^o, 70^o, 90^o, 110^o, 130^o$
Data Modulation	BPSK
Antenna spacing between elements, d	$\lambda/2$
Optimal weight technique	MMSE

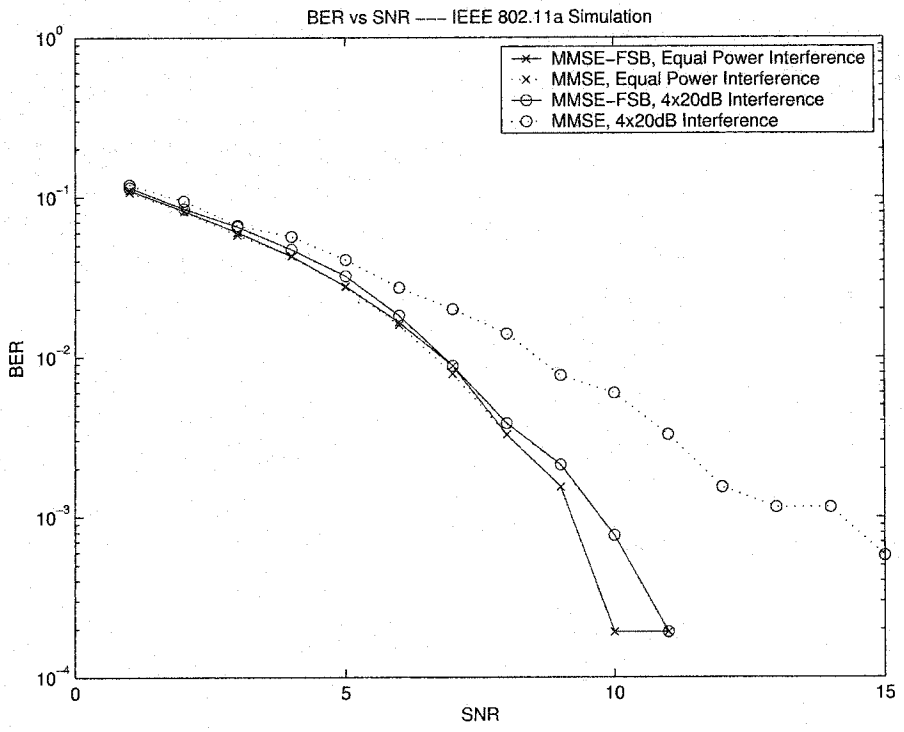

Figure 5.11: BER vs SNR, using IEEE 802.11a specifications

5.2 Channels with Rayleigh Fading

In this section a Rayleigh fading channel is studied. Two simulations are conducted to determine how the FSB algorithm responds to this environment. The first simulation assumes a linear time variant channel where each transmitted OFDM symbol in the data block experiences an independent fade. Typically this simulation is not realistic, but it shows the outer extremes for this particular channel. The second simulation assumes a linear time invariant channel where the entire transmitted OFDM data block is subjected to a single Rayleigh fade, meaning that each transmitted sample in the block experiences the same fade. This represents the other extreme in a fading channel.

The received OFDM signal presented in Eqn. (4.11) is updated for the case where a Rayleigh fade is experienced by each transmitted sample. The received signal is now given by,

$$y_{m,l} = \sum_{n=0}^{N-1} H_l x_n e^{jm2\pi \frac{f_n}{c} d\cos(\phi)} e^{j2\pi(\frac{ln}{NT_s}+f_o)t} + b_{m,l} \tag{5.1}$$

where $m = 0, 1, \ldots, M-1$, H_l represents the Rayleigh fading experienced by the l^{th} transmitted sample, f_n is given in Eqn. (4.6) and $b_{m,l}$ represents the AWGN of the l^{th} sample. Note Eqn. (5.1) represents the received signal for one user. The parameters used in this simulation are described in Table 5.1, with the following changes, four interfering powers of equal strength as the desired user and 6dB greater then the desired user are implemented for each simulation. A randomly chosen Rayleigh fade was simulated for individual transmitted samples in each block of data and complete channel knowledge is assumed at the receiver.

The BER plots in Figure 5.12 show that the MMSE algorithm provides some improvement in bit error performance compared to the MMSE-FSB algorithm, for both iterations of the simulation. However this performance improvement is small. The time variant channel alters the frequency bins of the received signal, therefore calibrating the weights to specific frequencies results in poorer performance of the MMSE-FSB technique. As stated before this channel is not realistic because the fading is usually reasonably constant over several sub-carriers.

Next consider a linear time invariant channel, which means that the channel varies at a slow enough rate that the channel is regarded as fixed during each block of data transmission. Here each transmitted OFDM symbol experiences the same fade. This model somewhat resembles burst type transmission, where each burst (or block) experiences the same fade. The time-invariant received signal is mathematically given by,

$$y_{m,l} = \sum_{n=0}^{N-1} H x_n e^{jm2\pi \frac{f_n}{c} d\cos(\phi)} e^{j2\pi(\frac{ln}{NT_s}+f_o)t} + b_{m,l} \tag{5.2}$$

where, H is the Rayleigh fade experience by all samples in the transmitted block of data.

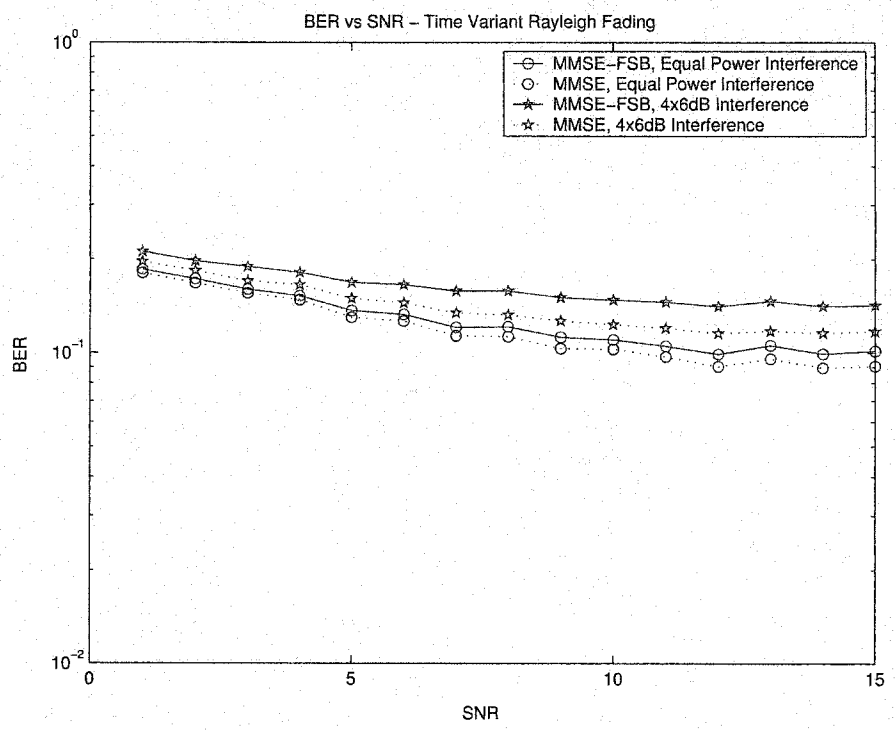

Figure 5.12: BER vs SNR, fading on each sub-carrier

Figure 5.13 shows the BER versus SNR for different levels of interference power in a time invariant channel. The MMSE-FSB technique shows small improvement when the power of the interfering signals is equal to the desired user. But larger performance improvements are seen in the case when the interfering power is 6dB and 12dB. This improvement is not as extreme as the improvement in an AWGN channel. Therefore these new results show that performance of the FSB algorithm is determined by three factors, 1) the power of the interfering signals, 2) the bandwidth of the system and 3) the channel response.

5.3 Scattering Model with an AWGN Channel

The FSB technique is now subjected to a scatter model based on a simplification of the concepts presented by Sayeed [27]. This model is developed as a bridge between the

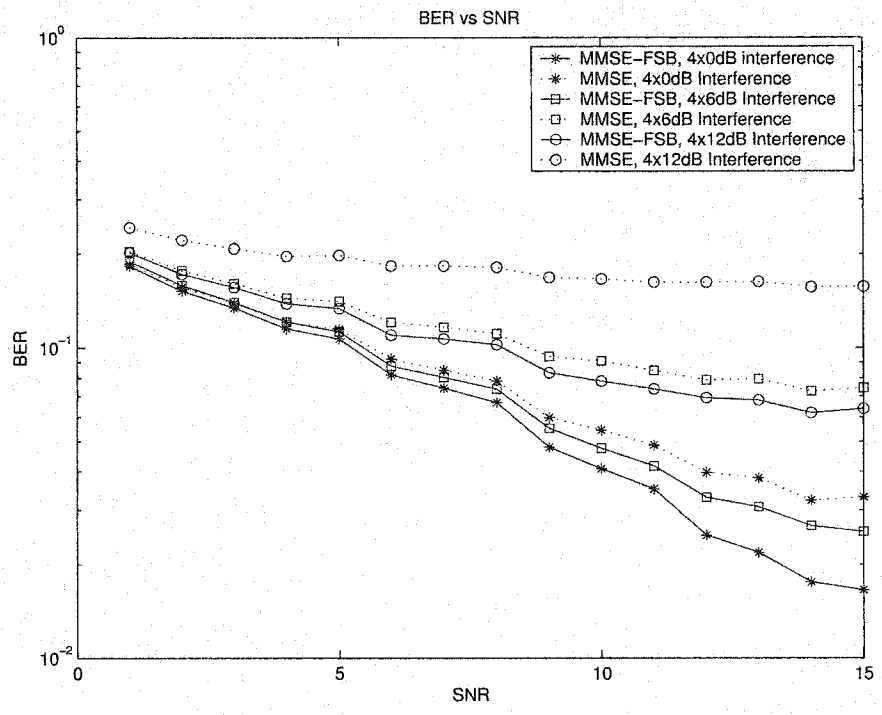

Figure 5.13: BER vs SNR, fading on each block of transmitted data

two extremes detailed in Section 5.2. A scattering cluster of received signals arriving with an angle spread of α is depicted in Figure 5.14. Assuming a limited angle spread, the received signal scatter clusters are averaged and normalized. This is simulated by averaging out the steering vector over all incoming signal spreads. For one user this is mathematically represented by

$$\tilde{\mathbf{s}}(\phi) = \frac{1}{\sqrt{s_c}}\mathbf{s}(\phi - \frac{\alpha}{2} + \varphi) + \ldots + \frac{1}{\sqrt{s_c}}\mathbf{s}(\phi + \frac{\alpha}{2} + \varphi) \tag{5.3}$$

where s_c represents the number of scattered received signals, ϕ represents the direction of arrival for the given user and φ represents a random phase. The steering vector, $\tilde{\mathbf{s}}(\phi)$ is normalized such that its first entry is unity.

Since the broadband steering vector is used to model the received signal in this example, Eqn. (5.3) is repeated for each sub-carrier and each user in the simulation.

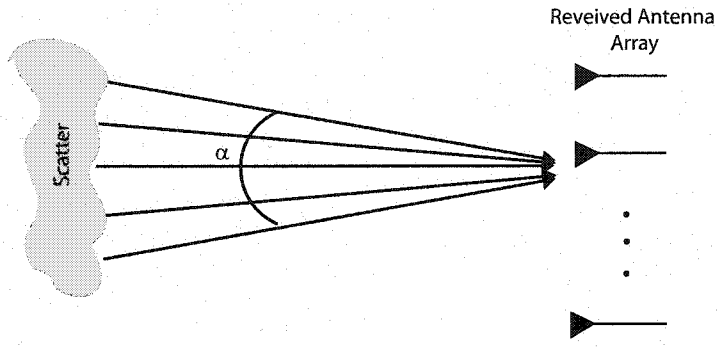

Figure 5.14: Scatter model at the received antenna array.

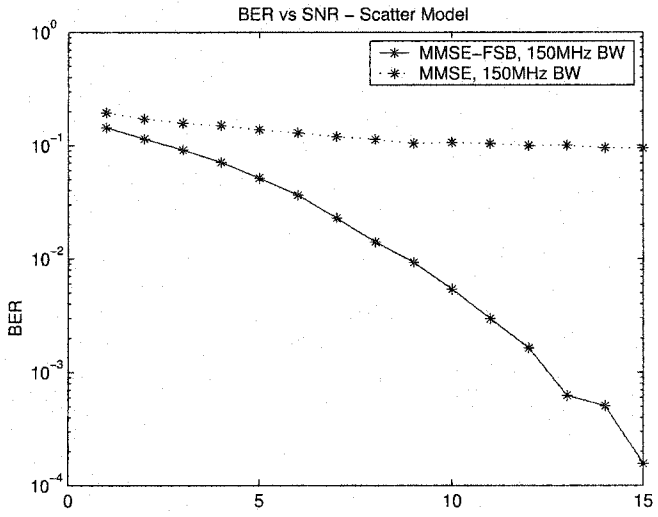

Figure 5.15: BER vs SNR, for scatter model with 4x12dB interference, and 150MHz bandwidth.

The simulations were carried out using parameters listed in Table 5.1 and fixing the interfering signals to 12dB. First a bandwidth of 150MHz was employed, Figure 5.15 shows the significant improvement in performance between the MMSE-FSB compared to MMSE. Figure 5.16 shows the effect of changing the OFDM bandwidth to 50MHz in the same simulation. As expected, a smaller improvement is noticed when a narrower bandwidth is used. Once again these simulations confirm what has been stated before.

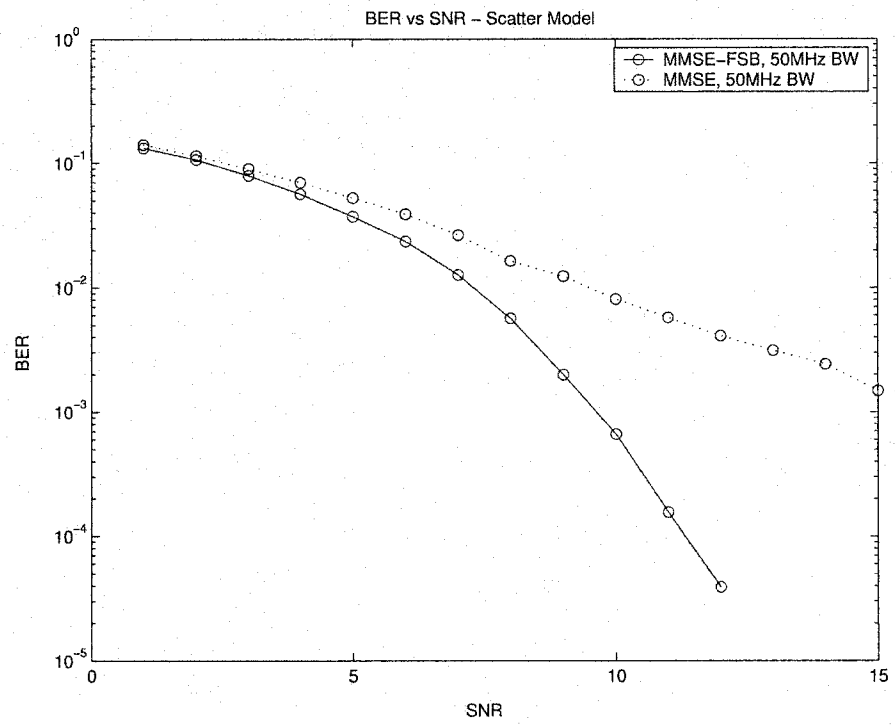

Figure 5.16: BER vs SNR, for scatter model with 4x12dB interference, and 50MHz bandwidth.

5.4 Wideband Beamformer versus FSB

Finally, in this section the FSB adaptive weight technique is compared to the wideband beamformer originally presented in Chapter 1.3.1. The wideband beamformer is a frequency-domain beamformer applied after the FFT and has been studied exclusively in

multi-path models [9] [10]. Here, we adapt the concepts of the wideband beamformer and apply them to a multi-user model. Clustering of sub-carriers has been proposed by Sun and Matsuoka to reduce the complexity of the wideband beamformer [9]. This concept is also applied in the virtual model.

The parameters used in this simulation are listed in Table 5.1, with the following changes presented in Table 5.3. The sub-carrier cluster sizes determine how many samples of the received data are used to estimate the correlation matrix for each cluster of the MMSE process. They also determine the number of narrowband beamformers used to form the wideband beamformer. For example, if the cluster size is chosen to be 32 sub-carriers in a system of 256 sub-carriers, then 8 narrowband beamformers are used to process the received data.

Table 5.3: Changes to System Parameters

Parameters	**Actual Values Used**
Strength of Interfering Users per Iteration	4×6 dB, 4×12 dB
Number of Sub-carriers per cluster	16, 32, 64, 128 and 256
Channel	AWGN

Figure 5.17 and Figure 5.18 show the comparison of the wideband beamformer versus the FSB algorithm when the interference is 4x6dB and 4x12dB respectfully. Notice that for smaller cluster sizes the wideband beamformer improves the bit error rate considerably. This is expected since the MMSE adaptive weight technique averages the power between the error of the received signal and the desired signal, therefore the weights are more specific over the cluster interval. When the interference is increased in Figure 5.18 the MMSE begins to diverge for quicker for larger cluster sizes. The MMSE-FSB algorithm remains relatively stable throughout.

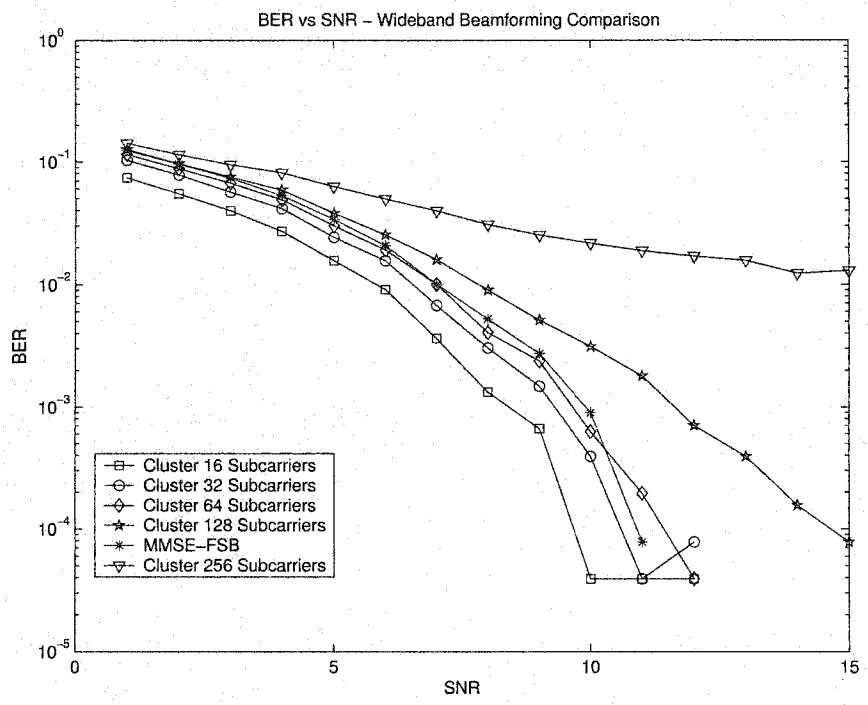

Figure 5.17: Wideband beamformer vs. FSB when interference is 4x6dB

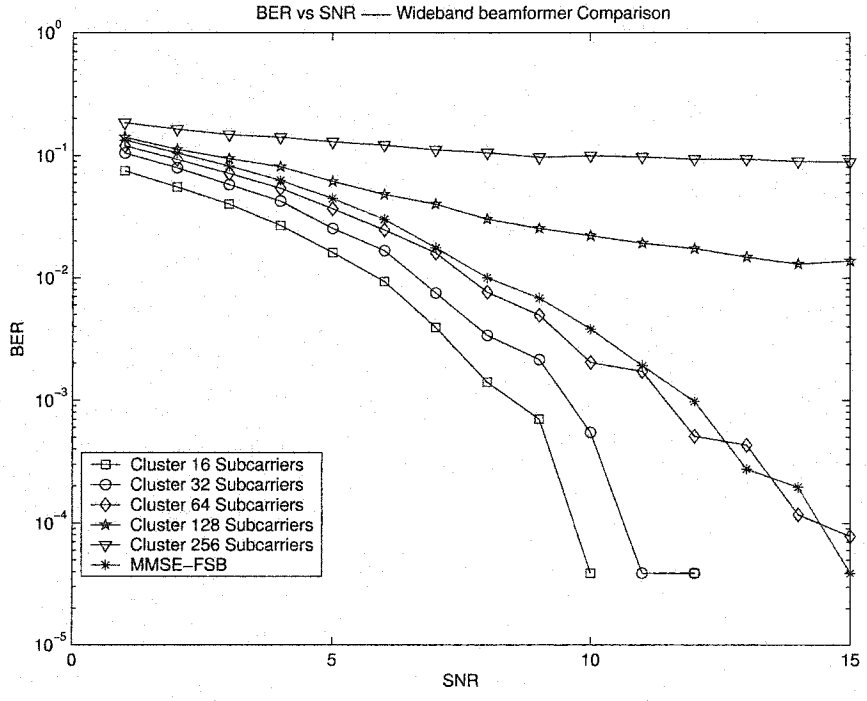

Figure 5.18: Wideband beamformer vs. FSB when interference is 4x12dB

5.5 Success or Failure of the FSB algorithm

This section identifies the reasons behind the successful simulations presented in the previous sections. Also a situation in which the FSB algorithm fails to improve performance in the system is examined. Three categories that contribute to the success or failure of this algorithm are:

1) Beampattern null placement and deviation

2) Number of interfering signals

3) Correlation

5.5.1 Null Deviation

Null deviation of classically determined weights for broadband signals is the main contributing factor to the degeneration in performance of the classical MMSE solution. A slight null deviation in a interference limited environment can have drastic effects on the performance of the system. The FSB algorithm ensures that the nulls remain fixed at the estimated interfering angles of arrival.

Consider a scheme where four 12dB interfering signals arrive with the following angles of arrival, $[50^o, 70^o, 110^o, 130^o]$. The rest of the parameters used in this simulation are listed in Table 5.1. Figures 5.19 to 5.22 compare the beampatterns of the first and last frequency in a broadband signal for MMSE and MMSE-FSB techniques. Figure 5.19 shows a slight null deviation between the beampatterns for MMSE determined weights, when a 150MHz bandwidth is used. Thus the nulls in the beampattern are not optimally placed to mitigate the stronger interfering signals and system performance suffers. Figure 5.20 shows the how the FSB algorithm behaves using the same parameters as Figure 5.19 for the simulation. Notice that the FSB algorithm fixes the nulls at the given incoming angels of arrival, ensuring that the optimality of the classical weight techniques for the center frequency is achieved for all frequencies.

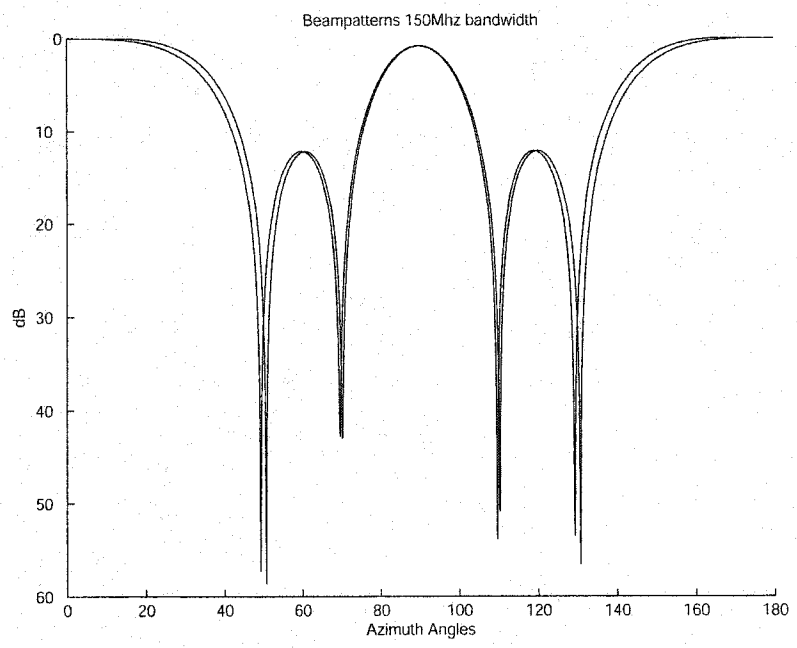

Figure 5.19: Beampatterns comparing the first and last frequencies in wideband signals, beampattern of MMMSE weights for a 150MHz OFDM system

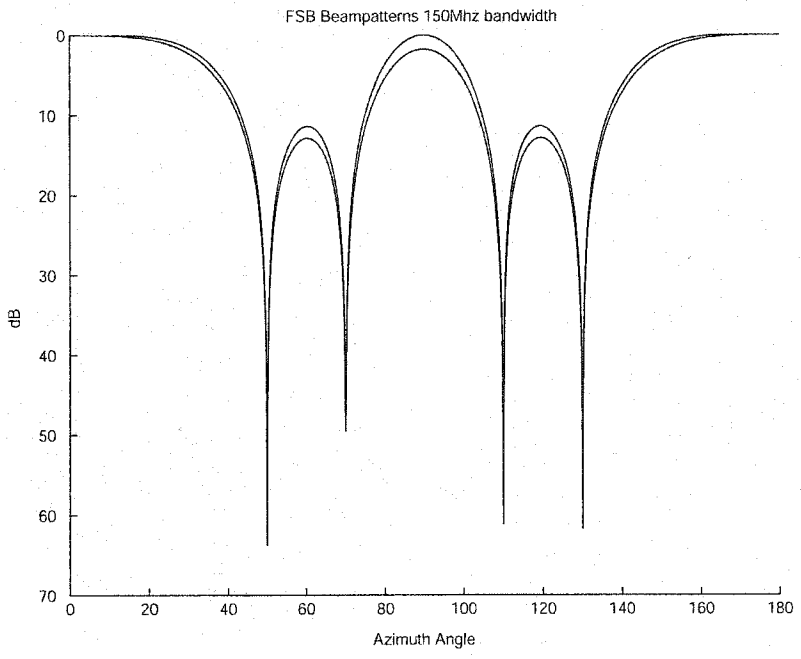

Figure 5.20: Beampatterns comparing the first and last frequencies in wideband signals, beampattern of MMSE-FSB weights for a 150MHz OFDM system

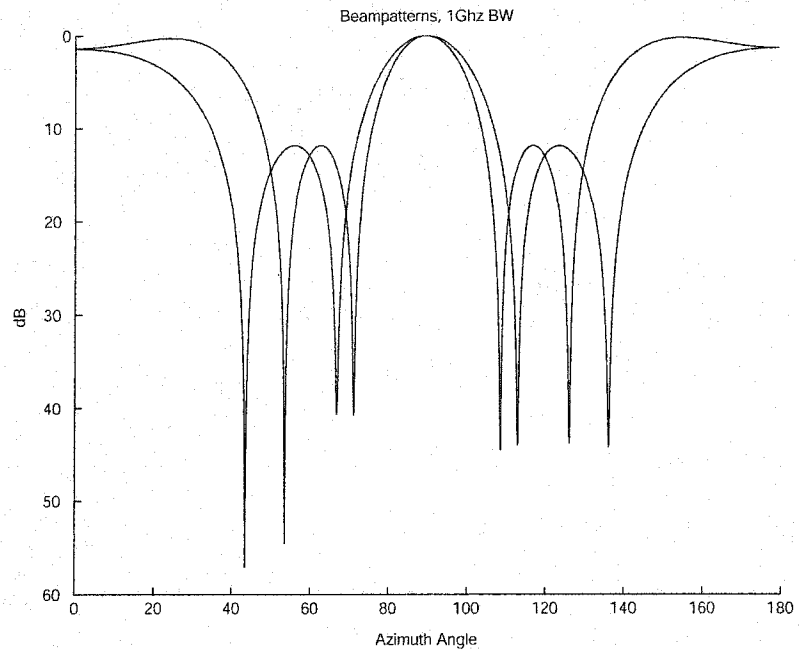

Figure 5.21: Beampatterns comparing the first and last frequencies in wideband signals, beampattern of MMSE weights for a 1GHz OFDM system

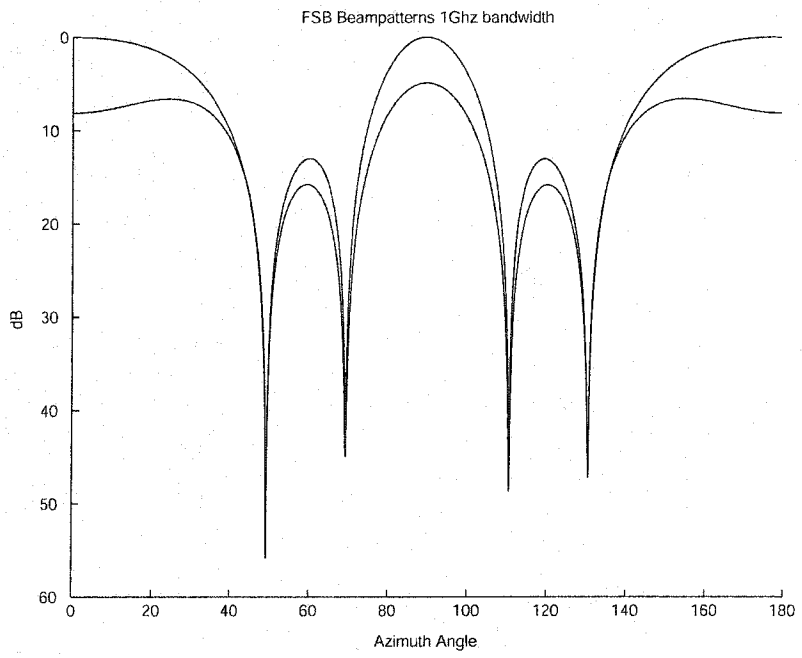

Figure 5.22: Beampatterns comparing the first and last frequencies in wideband signals, beampattern of MMSE-FSB weights for a 1GHz OFDM system

5.5.2 Number of Interfering signals

The success of the FSB algorithm depends on the success of the optimal weight technique. As noted in chapter 3, an M-element adaptive array can only place M-1 nulls in the direction of interfering signals. If more than M-1 signals interfere with the desired signal, optimal weight techniques cannot suppress the interference, resulting in failure of the FSB algorithm as well. In practical situations no more than two or three signals that reside in the same channel interfere with the desired signal, but as more devices are becoming wireless this situation may change.

5.5.3 Correlation

All the previous simulations assumed that the adaptive antenna array was completely correlated. Beamforming techniques are the ideal choice for array processing in such circumstances. If an uncorrelated adaptive arrays is implemented, diversity schemes excel over beamforming techniques. The remaining portion of the chapter shows how the FSB algorithm fails completely when the channel is uncorrelated. Its performance is significantly worse then classical beamforming techniques alone. Reasons for this failure in system performance is based on the fact that the uncorrelated channel offsets the frequency bins. The following simulations will compare beamforming schemes.

5.6 Simulation of the uncorrelated model

The goal of this section is to examine the effect that correlation between antenna elements has on the FSB algorithm. In previous models and simulations it was assumed that the spatial fading between received signals at each element is completely correlated with the other elements. It was also previously suggested that diversity techniques should be implemented in totally or effectively uncorrelated models. However in realistic environments correlation is somewhere in between the two extremes. The degree of cor-

relation between antenna elements is determined by the channel, the physical location of the antenna with respect to scatters and the parameters of the array such as element spacing [8].

For this simulation a simplified version of the one ring model was used to model the correlation between antenna elements. Let ρ represent the correlation of fades between an M-element received antenna array. Assuming a linear time-invariant channel, the channel impulse response (CIR) $\mathbf{c} = [c_0, c_1, ..., c_{M-1}]^T$, is given by,

$$\mathbf{c} = \mathbf{R}^{1/2}\mathbf{h} \tag{5.4}$$

where,

$$\mathbf{R} = \begin{bmatrix} 1 & \rho & \cdots & \rho \\ \rho & 1 & \cdots & \rho \\ \vdots & \vdots & \ddots & \vdots \\ \rho & \rho & \cdots & 1 \end{bmatrix}, \tag{5.5}$$

$$\mathbf{h} = [h_0, h_1, \cdots, h_{M-1}]^T, \tag{5.6}$$

Here, $\mathbf{R}$ is the $M \times M$ correlation matrix, $\mathbf{h}_m$ is a vector of uncorrelated Rayleigh fading terms.

Next consider an M-element, N sub-carrier OFDM system. The l^{th} sample received at the m^{th} antenna, $y_{m,l}$, is given by,

$$y_{m,l} = \sum_{n=0}^{N-1} c_m x_n e^{jm2\pi \frac{f_n}{c} d\cos(\phi)} e^{j2\pi(\frac{ln}{NT_s}+f_o)t} + b_{m,l} \tag{5.7}$$

where, $m = 0, 1, \cdots, M-1$ represents the antenna element, c_m is the CIR given in Eqn. (5.5), x_n is the frequency-domain data that is originally transmitted and $b_{m,l}$ represents the AWGN of the l^{th} sample. Notice the received signal represents one user. For

a multi-user system, Eqn. (5.5) and Eqn. (5.8) are recreated for each user and summed to create the overall received signal.

Figure 5.23 shows the BER versus SNR of the uncorrelated model using parameters described in Table 5.1. The received signals are assumed to be totally uncorrelated between antenna elements ($\rho = 0$). In most standards $\rho \leq 0.5$ is considered to be uncorrelated. Notice the MMSE-FSB algorithms unstable performance in an uncorrelated channel. Since BPSK modulation was used the FSB's performance is no better then randomly choosing 1 or -1. Although the MMSE alone does not provide ideal weights for this type of scenario, performance is significantly better then the MMSE-FSB technique. The reason the FSB algorithm fails is because the uncorrelated signals combined with the random Rayleigh channel have a strong effect on the frequency bins causing an offset. Therefore trying to optimize weights for specific frequency bins adds inter-channel interference between carriers.

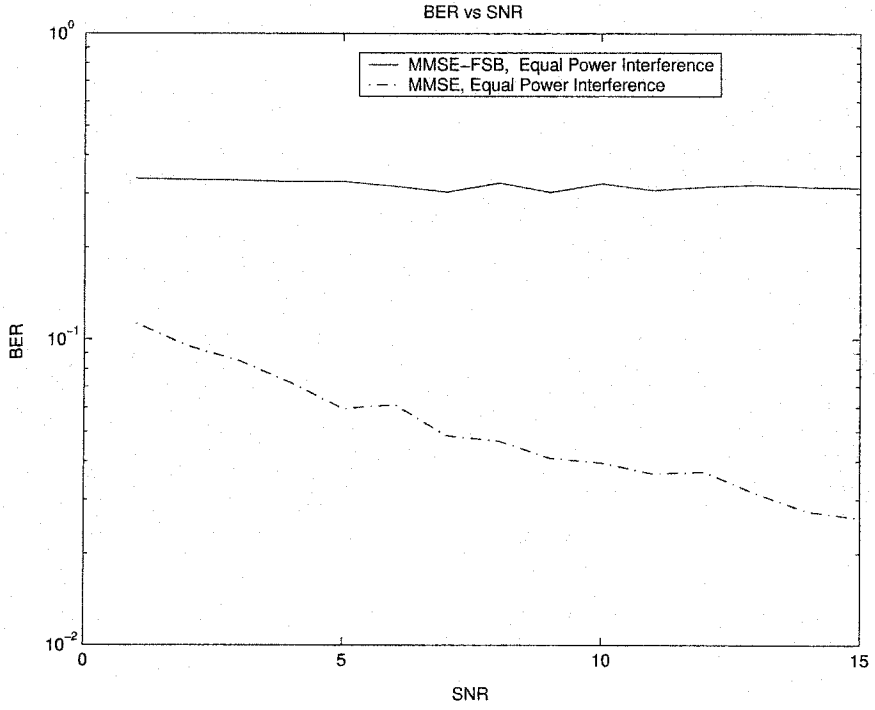

Figure 5.23: BER vs SNR, Uncorrelated received signals

Figure 5.24 compares the BER versus correlation between antenna elements. In this simulation the SNR was fixed at 10dB and the remaining parameters used are listed in Table 5.1. This figure shows that the FSB algorithm begins to show improvement in system performance when $\rho > 0.6$. The regression of the FSB algorithm is observed in the uncorrelated portion of the graph (i.e. $\rho \leq 0.5$). Therefore the FSB algorithm is only applicable in highly correlated systems and diversity schemes should be implemented in uncorrelated systems as before.

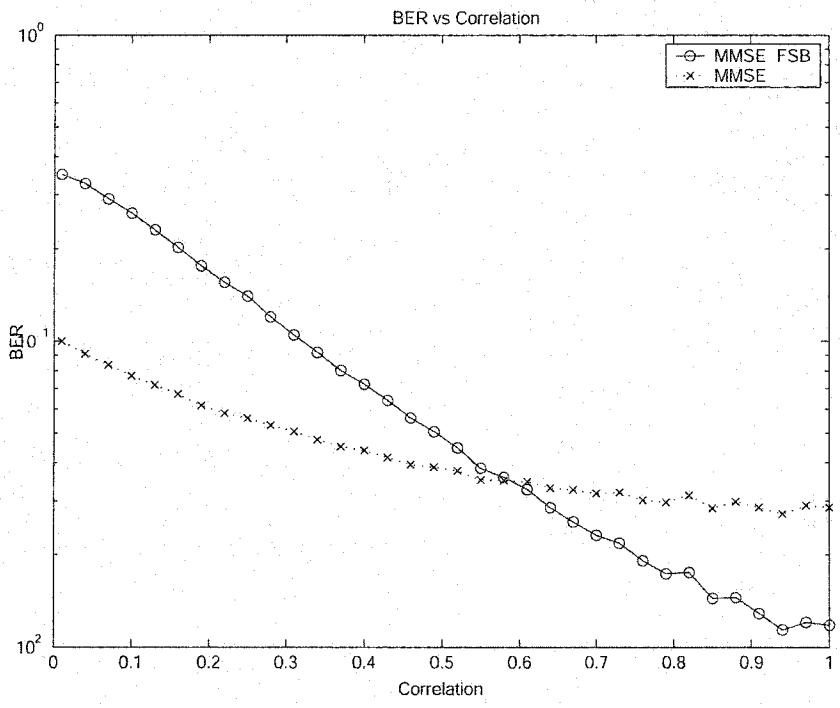

Figure 5.24: BER vs Correlation

5.7 Summary

Simulations to test the limits of the FSB algorithm were investigated in this chapter. The AWGN model showed that the performance of the FSB algorithm improves with stronger interference and also larger bandwidths of the OFDM model. In this simulation

increasing the number of sub-carriers had an improved effect on FSB's performance, and degenerated the MMSE's performance, eventually reaching a floor. Next Rayleigh fading was added to the correlated model. MMSE performance was slightly better then MMSE-FSB in a time-variant channel. In a time-invariant channel the MMSE-FSB performance improved for larger interfering signals, but the improved performance was significantly less then the AWGN channel. The reason for the improved performance was shown to be due to the null divergence in the classically determined weights. For very large broadband systems a significant increase in null deviation was observed for the MMSE weight technique, while the FSB algorithm preserved the null locations, therefore increasing the performance. Finally the correlation model was presented and showed that the FSB weight technique fails completely in uncorrelated systems.

Chapter 6

Conclusion and Future Work

6.1 Conclusion

OFDM has gained considerable momentum in recent years and is becoming a standard to which all broadband communication systems can be compared. Many characteristics of OFDM make it attractive such as its ability to achieve high data rates, efficient use of spectrum and immunity to frequency selective fading. However, as more devices become wireless and because of limited frequency band allocations worldwide, stronger interference will become more of an obstacle in future systems. To manage this dilemma an innovative and low computational solution was introduced.

The FSB algorithm is an extension to classical adaptive weight techniques. Through rigorous simulations it was discovered that the FSB algorithm increases the performance of highly correlated OFDM systems. Three parameters determine how successful the performance improvement will be, the strength of the interfering signals, the size of the OFDM bandwidth and the channel response. The improved performance is based on null deviation in the classically determined weights between adjacent frequency bins in broadband systems. In an interference-limited environment this could mean significant performance loss. Larger bandwidths produce larger null deviations; therefore weaker

interference will be needed to overcome the deviated nulls. Simulations also showed that the FSB algorithm becomes unstable in uncorrelated or slightly correlated fading scenarios. The uncorrelated system model shifts the location of known frequency bins, rendering the known frequency information useless.

6.2 Future Work

The following is a list of potential areas related to the research that can be pursued and might provide interesting results for future work.

- All the discussions focused on the basic OFDM system, it would be interesting to apply the broadband steering vector and the FSB algorithm to other OFDM based systems, such as MC-CDMA, OC-OFDM and MC-DS CDMA.
- The FSB algorithm in this research could be made less computational by frequency clustering. Since the steering vectors exhibit minimal changes over small bandwidths.
- In uncorrelated systems it could be possible to track the offset caused by the channel by assuming complete channel information and adjust weights specific to the offset frequencies.
- The beamforming technique chosen for comparison was direct matrix inversion MMSE. It would be interesting to apply the FSB algorithm to iterative (LMS and RLS), and blind (CMA) adaptive weight techniques to investigate how they compare to each other.
- Throughout this simulation perfect frequency knowledge, channel knowledge and timing synchronization were assumed to be known at the receiver. Frequency offset, channel estimation and time synchronization continue to be large and active areas of research. It would be interesting to see how the FSB algorithm reacts to these changes.

- The beampatterns were restricted to one axis, and the steering vector was determined for the equi-spaced uniform linear array. It would be interesting to simulate the FSB algorithm in a circular or planar antenna array and investigate 3D beampatterns.
- Last but not least, it would be useful to actually build a working DSP chip-set of the proposed algorithm and investigate its performance in field trials.

Bibliography

[1] A. L. Intini, "Orthogonal frequency division multiplexing for wireless networks," tech. rep., University of California, UCSB Center for Research in Electric Art Technology, December 2002. http://www.create.ucsb.edu/ATON/01.01/OFDM.pdf.

[2] A. Pandharipande, "Principles of OFDM," *IEEE Potentials*, vol. 21, no. 2, pp. 16–19, 2002.

[3] T. J. Lim, "An introduction to multicarrier modulation," tech. rep., A CWC Technical Report, University of Toronto, June 1998. http://www.comm.utoronto.ca/ limtj.

[4] J. Heiskala and J. Terry, *OFDM Wireless LANs: A Theoretical and Practical Guide.* Sams Publishing Inc., 2001.

[5] L. Hanzo, "Bandwidth-efficient wireless multimedia communications," *Proc. IEEE*, vol. 86, pp. 1342–1382, November 1998.

[6] R. V. Nee, "A new OFDM standard for high data rates wireless lan in the 5GHz," *Proc. of IEEE VTC, IEEE VTS 50th*, vol. 1, pp. 258–262, Sept 1999.

[7] N. Prasad and H. Teunissen, "A state-of-the-art of Hiperlan/2," *Proc. of IEEE VTC, IEEE VTS 50th*, vol. 5, pp. 2661–2666, Sept. 1999.

[8] J. C. Liberti and T. S. Rappaport, *Smart Antennas for Wireless Communications: IS-95 and Third Generation CDMA Applications.* Upper Saddle River, New Jersey: Prentise-Hall, Inc., 1997.

[9] Y. Sun and H. Matsouka, "A novel adaptive antenna architecture - sub-carrier clustering for high speed OFDM systems in presence of rich interference," *VTC*, vol. 3, pp. 1564–1568, Spring 2002.

[10] B.-L. Cheung, F. Alam, J. H. Reed, and W. D. Woerner, "A new beamforming algorithm for OFDM systems," *In the Proceedings of the 14th Annual International Conference on Wireless Communications*, July 2002.

[11] D. Gerakoulis and P. Salmi, "An interference suppressing OFDM system for ultra wide bandwidth radio channels," *IEEE Conference on Ultra Wideband Systems and Technologies*, pp. 259–264, May 2002.

[12] D. Gerakoulis and P. Salmi, "An interference suppressing OFDM system for wireless communications," *IEEE Conference on Communications (ICC)*, vol. 1, pp. 259–264, May 2002.

[13] M. Munster and L. Hanzo, "Co-channel interference cancellation techniques for antanna array assisted multiuser OFDM systems," *3G Mobile Communication Technologies*, pp. 256–260, March 2000.

[14] Y. Li and N. R. Sollenberger, "Adaptive antenna arrays for OFDM systems with cochannel interference," *IEEE Transactions on Communications*, vol. 47, pp. 217–229, Feb. 1999.

[15] M. Toeltsch and A. F. Molisch, "Equalization of OFDM-systems by interference cancellation techniques," *Internation Conference on communications (ICC)*, vol. 6, pp. 1950–1954, June 2001.

[16] S. Kapoor, D. J. Marchok, and Y.-F. Huang, "Adaptive interference surppression in multiuser wireless OFDM systems using antenna arrays," *IEEE transactions on signal processing*, vol. 47, pp. 3381–3391, December. 1999.

[17] J. Kim and J. M. Cioffi, "Spatial multiuser access OFDM with antenna diversity and power control," *Proc. of IEEE VTC, IEEE VTS 52nd*, vol. 1, pp. 273–279, Fall 2000.

[18] L. C. Godara, "Applications of antenna arrays to mobile communications part 2: Beam-forming and direction of arrival considerations," *Proceeding of IEEE*, vol. 85, pp. 1195–1245, August 1997.

[19] B. R. Salzberg, "Performance of an efficient parallel data transmission system," *IEEE Transactions on Communications*, vol. COM-15, pp. 805–813, December 1967.

[20] S. B. Weinstein and P. M. Ebert, "Data transmission of frequency-division-multiplexing using Discrete Fourier Transform," *IEEE Transactions on Communications*, vol. COM-19, pp. 628–634, October 1971.

[21] B.-L. Cheung, "Simulation of adaptive array algorithms for OFDM and adaptive vector OFDM systems," tech. rep., Virgina Polytechnic Institute and State University, Masters Thesis, Sept 2002. http://scholar.lib.vt.edu/theses/available/etd-09042002-142835/unrestricted/OFDMbeamforming.pdf.

[22] L. C. Godara, "Applications of antenna arrays to mobile communications part 1: Performance, improvement, feasibility, and system considerations," *Proceeding of IEEE*, vol. 85, pp. 1031–1060, July 1997.

[23] S. Haykin, *Adaptive Filter Theory.* Prentice-Hall, 1996.

[24] Y. Lee and N. R. Sollenburger, "Adaptive antenna arrays for ofdm systems with co-channel interference," *IEEE Transactions on Communications*, vol. 47, pp. 217–229, Feb. 1999.

[25] C. K. Kim, K. Lee, and Y. S. Cho, "Adaptive beamforming algorithm for OFDM systems with antenna arrays," *IEEE Transactions on Consumer Electronics*, vol. 46, pp. 1052–1058, Nov. 2000.

[26] Y.-C. Liang and F. Chin, "Downlink channel covariance matrix (DCCM) estimation and its applications in wireless ds-cdma systems," *IEEE Journal on selected areas in Communications.*, vol. 19, pp. 222–232, Feb 2001.

[27] A. M. Sayeed, "Deconstructing multiantenna fading channels," *IEEE Transactions on Signal Processing*, vol. 50, pp. 2563–2579, October 2002.